VirginiaTech
Invent the Future

**VIRGINIA POLYTECHNIC INSTITUTE
AND STATE UNIVERSITY**

The Charles E. Via, Jr. Department
of Civil and Environmental Engineering
Blacksburg, VA 24061

Structural Engineering and Materials

ENERGY DISSIPATION OF
COLD-FORMED STEEL CONNECTIONS

by

Andreas Haus

Report No. CE/VPI-ST-14/02

January 2014

Energy Dissipation for Cold Formed Steel Connections

Energiedissipation in Anschlüssen von kaltgeformten Stahlprofilen

Master Thesis von Andreas Haus

TECHNISCHE
UNIVERSITÄT
DARMSTADT

Table of Contents

List of Figures

List of Tables

Acronyms

#33	Connection 0.88 mm to 0.88 mm
#44	Connection 1.15 mm to 1.15 mm
#103	Connection 2.58 mm to 0.88 mm
AISI	American Iron Steel Institute
AISI S	American Iron Steel Institute Standard
CFS	Cold-Formed-Steel
CUREE	Consortium of Universities for Research in Earthquake Engineering
EEEP	Equivalent Energy Elastic Plastic Curve
FEMA	Federal Emergency Management Agency
FPH	Flatpan Head
F_u	Ultimate Stress
HEX	Hex Washer Head
M	Moment
M_n	Predicted Nominal Moment
MTS	Material Testing Systems
OSB	Oriented Strand Board
P	Load
PCH	Pancake Head
P_n	Predicted Nominal Load
TRU	Truss Head
WF	Web-to-Flange
WW	Web-to-Web
d'_w	Effective Pull-Over Diameter
e	Eccentricity
t_1	Thickness of Upper Stud
t_2	Thickness of lower Stud
w	Displacement
Δ	Displacement
Δ_{mon}	Displacement Monotonic Test

1. Introduction

1.1. Motivation

Compared to Germany, cold-formed steel constructions become a more and more common application in the United States of America. Especially in high seismic regions, cold-formed steel is an alternative to traditional applications like hot-rolled steel and reinforced concrete. On the construction side, cold-formed steel constructions have an economic advantage over concrete construction as a result of faster and lighter building. These advantages in constructing have an influence on the behavior of the construction under seismic load. While traditional systems use controlled local yielding for energy dissipation, cold-formed steel framing uses subsystem deformation and interaction.[1]

Picture 1.1.1. – A typical cold-formed steel application

---

[1] Padilla, D., Cyclic Energy Dissipation of Cold-Formed Steel Studs - Experiencing Euler Buckling.

The characteristic of cold-formed steel framing is constructing with thin walled members. Like in wood framing, in cold-formed steel framing screws without nuts are used as a connection. Therefore the performance of cold-formed steel connections is different to the common hot rolled steel constructions. The reduced thickness of the steel framing members enables connections via screw tilting next to bearing and tearing.

In 2004, the test series *Performance of steel frame / wood sheathing screw connections subjected to monotonic and cyclic loading*[2] was conducted by A. Okasha at McGill University. In this test series steel to sheathing tests were done. The objective of this research was to provide information on connection performance of steel frame / wood panel shear walls under cyclic loading and to show the influence of different sheathing types, different thicknesses and different orientations on their behavior.

In 2012 K. D. Peterman also conducted a test series with steel to sheathing connections. In this test series she tested oriented strand board (OSB) and gypsum sheathings to steel.[3] It can be seen that a small range of steel to sheathing research already exists. The behavior of a pure cold-formed steel-to-steel connection under cyclic load is nearly unexplored.

1.2. Objectives and Scope

At the current state of science there is no experience of the loading capacity for cold-formed steel connections under cyclic load. To get a better understanding of the performance of different screws in cold-formed steel connections, an extensive test series with different screw heads and sizes must be done.

The first part of this research is the comparison of different screw heads. Therefore a test series with 48 tests was conducted. These tests include two different orientations of the connection members, different thicknesses of the members and different heads of the screws. For the test matrix of the monotonic test series please refer to the test matrix in chapter 4. The objective of this first part of the research is to show the different behavior of the screws and the influence of the boundary conditions of the different connections.

---

[2] Okasha, A., Performance of steel frame / wood sheathing screw connections subjected to monotonic and cyclic loading.

[3] Peterman, K.D., Nakata, N., Schafer, B.W., Cyclic Behavior of Cold-Formed Steel Stud-to-Sheathing Connections.

The second part of this research is about the influence of cyclic load on the behavior of a cold-formed steel connection. Therefore a test series under monotonic load with 54 tests and a test series under cyclic load with also 54 tests was conducted. The variables in these test series were the thicknesses of the members, the orientation of the members and the size of the screws. The final test matrixes for the monotonic and cyclic tests can be seen in chapter 5. The objective is to determine the behavior of different screw sizes under cyclic loading and to figure out the difference of the screws under monotonic load and of the screws under cyclic load.

1.3. Background

1.3.1. Cyclic Testing

The idea behind cyclic testing is to get knowledge about the energy dissipation of a connection under cyclic loading. In 2004 a test series of steel frame / wood sheathing screw connections was conducted by A. Okasha. The scope of this research was to analyze the influence of different types of screws, of different sheathing material and of different orientations of the connection. For A. Okasha's research a monotonic and a cyclic study was conducted. The monotonic tests were conducted under tension with a constant cross-head loading rate of 2 mm/min until the post-peak load reached 50% of the peak load of the current test. For the reversed cyclic test the CUREE protocol (2001) was used.[4]

The monotonic tests were important to get the reference deformation for the cyclic protocol. A detailed description of the CUREE protocol follows in chapter 1.3.2.

For the evaluation of the monotonic tests an energy elastic-plastic curve (EEEP) was used. The method approximates the nonlinear load-displacement curve of the steel to sheathing

---

[4] Okasha, A., Performance of steel frame / wood sheathing screw connections subjected to monotonic and cyclic loading.

connection by an ideal bilinear equivalent curve.[5] This curve can be compared with another EEEP of the cyclic tests, which is based on the backbone of the cyclic load displacement plot.

The results of the tests show a significant influence to the load displacement behavior of the sheathing type and edge distance. Good results were reached by an edge distance of 12.5mm. The results of the cyclic tests are non symmetric and show a higher maximum load on the compression side compared to the tension side.

Another interesting test series was conducted by K.D. Peterman. Like the research of A. Okasha, this research was about the cyclic behavior of stud-to-sheathing connections and also uses the CUREE cyclic protocol. The results of this research vary with the used specimen. While OSB specimens behave symmetrically, specimens of gypsum show a non-symmetric behavior for tension and compression.

The AISI Standard AISI S905 "Test methods for mechanically fastened cold-formed steel connections" advises tension tests for standard cold-formed steel connections, but does not give any advice for cyclic tests.

Because of the different test methods, the use of the CUREE protocol should not transferred one to one to a steel-to-steel setup. The following chapter discusses the differences of the cyclic loading protocols and provides details of the protocol used in this thesis.

1.3.2. Existing Loading Protocols

The knowledge of the maximum strength and the maximum deformability of an element is a requirement for safe and economical construction. For static calculation under constant load, sufficient data usually is available to compare the load with the resistance including safety factors. For new materials or extraordinary loads, in example in an earthquake, we often do not know the characteristics of such materials or such an event. In order to design structures that are economic and able to resist extreme forces, proper simulations and testing is necessary. In earthquake engineering, strength and deformation capacities depend on cumulative damage, which implies that every component has a permanent memory of past

---

[5] Okasha, A., Performance of steel frame / wood sheathing screw connections subjected to monotonic and cyclic loading.

damaging events. It further implies that at any instance in time the component will remember all past excursions that have contributed to the deterioration in its state of health.[6] In light of the above, it is essential that a loading protocol has to replicate the load and deformation history of an earthquake. The objective at this juncture should be to characterize hysteretic behavior and associated progression of damage states rather than reproducing seismic demands for a specific configuration.[7]

One of the main challenges in learning from historic data is that every earthquake is a unique seismic event, which won't repeat itself under identical conditions. As a result, a unique or best loading protocol for every configuration does not exist. Each protocol tries to imitate any future unknown earthquake as good as possible.

At present state, there are several different protocols. They all try to replicate a seismic event to their best knowledge and show several differences, whereas the differences are mainly in detail rather than in concept.[8] Table 1.3.2.1 gives an overview of the loading protocols that have been developed during the past 20 years. It can be seen that most of the protocols are based on certain materials, which mainly are steel or wood.

Protocol	Material
ATC-24 Protocol (ATC-24, 1992)	Steel
SAC Protocol (Clark et al., 1997)	Steel
SPD Protocol (Porter, 1987)	Wood / Masonry
CUREE (Krawinkler et al., 2000-b)	Wood / Steel
ISO (ISO, 1998)	Wood
FEMA 461 (FEMA 2007)	-

Table 1.3.2.1. – Overview of different protocols last 20 years[9]

---

[6] Krawinkler, H., Loading Histories for cyclic tests in support of performance assessment of structural components.

[7] Padilla, D., Cyclic Energy Dissipation of Cold-Formed Steel Studs – Experiencing Euler Buckling.

[8] Krawinkler, H., Loading Histories for cyclic tests in support of performance assessment of structural components.

[9] Krawinkler, H., Loading Histories for cyclic tests in support of performance assessment of structural components.

This study takes a closer look of the CUREE and the FEMA 461 protocols. Okasha and Peterman have used the CUREE protocol for their test series, and the FEMA 461, which is not developed for a specific material, was the basis for the cyclic test series in this paper.

CUREE

The CUREE protocol was developed by Krawinkler et al in 2000. It is usually used for sheathing and steel to sheathing tests. But it was also used for steel to steel tests in the past. The specific of the CUREE protocol are the "trailing" cycles. Trailing cycles are smaller cycles which follow the preceding larger, called "primary", cycles. Picture 1.3.2.1 shows on the left side an example of a CUREE protocol where the trailing cycles can be seen.

The amplitude of the cycles is based on a reference displacement Δ. This displacement Δ is a measure of the deformation capacity of the specimen. So it is common to calibrate this displacement by running monotonic or near-fault tests first. It is suggested to use a reference displacement $\Delta = 0,6\Delta_{mon}$ for the cyclic tests.[10]
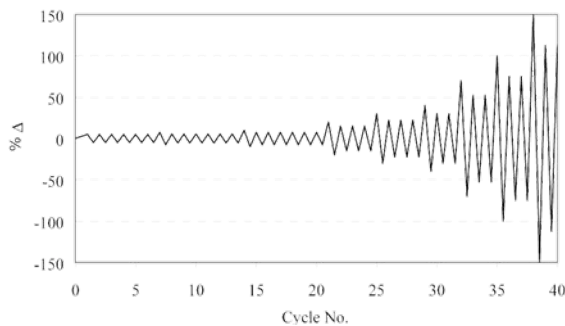
CUREE   FEMA 461
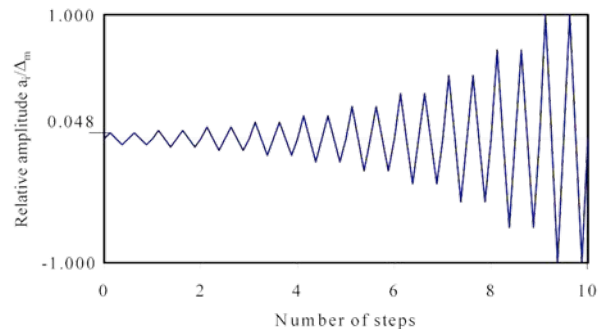
Picture 1.3.2.1. – Comparison of the CUREE and the FEMA 461 protocols

FEMA 461

The FEMA 461 protocol is a quasi-static cyclic protocol[11] and was developed for testing of drift sensitive nonstructural components, but is applicable in general also to drift sensitive

---

[10] Krawinkler, H. Parisi, F., Ibarra, L., Ayoub, A., Medina, R., Development of a Testing Protocol for Woodframe Structures.

[11] Applied Technology Council, Interim Testing Protocols for Determining the Seismic Performance Characteristics of Structural and Nonstructural Components.

structural components[12]. As it can be seen in picture 1.3.2.1 on the right side, the FEMA 461 protocol does not use trailing cycles. After two cycles with the same amplitude, the amplitude of the deformation increases.

Like for the CUREE protocol, the amplitude Δ is based on a deformation out of monotonic tests.

1.3.3. Plate Theory

As mentioned above, the loading protocol is based on a reference displacement Δ. It is very time-consuming to get this reference displacement out of tests and especially for large projects it is not productive enough. Another, and faster way to get this displacement, is to calculate it. The basis for the calculation can be seen in picture 1.3.3.1.
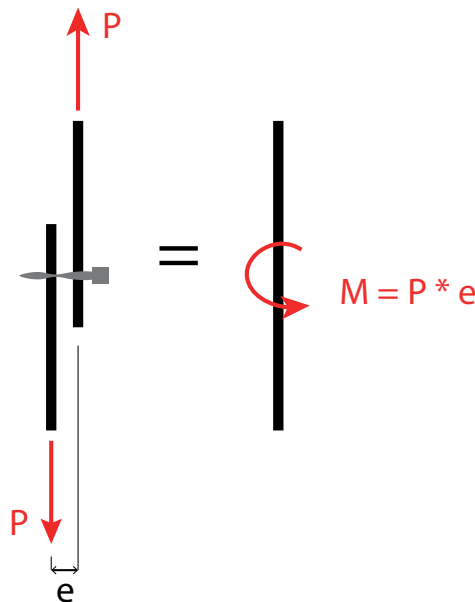
Picture 1.3.3.1. – Relation of Load and Moment

The used test setup consists out of two plates, which are connected with a screw. Because of the thickness of the plates, the centerlines, which are the way the load follows, have a small eccentricity called e. The outcome of the eccentricity e and the load P is the moment M.

---

[12] Krawinkler, H. Loading histories for cyclic tests in support of performance assessment of structural components.

If we simplify the system on the left side of picture 1.3.3.1 now, we get a plate with a concentrated load like it is shown in picture 1.3.3.2. There can be found a lot of already solved equations for a plate under load in the literature.
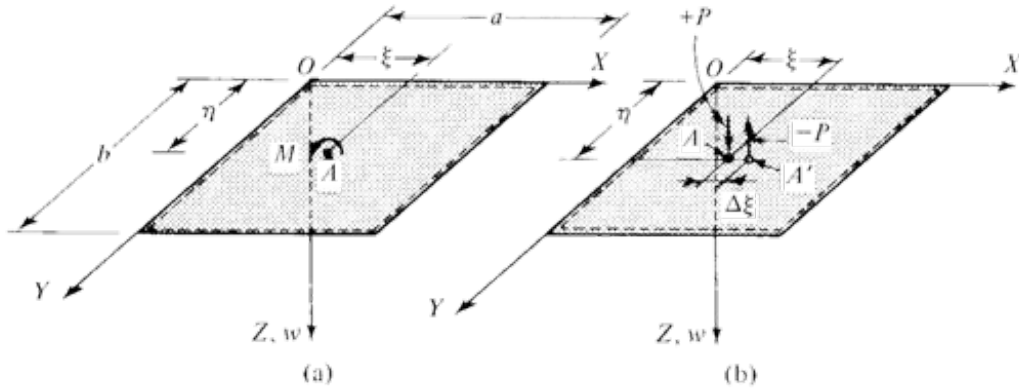
Picture 1.3.3.2. – Concentrated Moment[13]

In his paper *Theory and Applications of Plate Analysis: Classical, Numerical and Engineering Methods*, Szilard provides an equation for a concentrated moment on a simply supported rectangular plate. It uses the Navier's method and is solved for a single moment at a point $A(\xi, \eta)$.

The solution for a plate under a concentrated moment can be obtained by replacing the moment by a fictitious couple P and P' with a distance $\Delta\xi$. So M can be written as $M = P \cdot \Delta\xi$. By decreasing $\Delta\xi \to 0$ while maintaining the original value of M, P must increase in the same way $\Delta\xi$ decreases. It follows that P can be replaced by M.

The solved equation of Szilard is as follows[14]:

$$w = \frac{4M}{\pi^3 a^2 bD} \sum_m \sum_n \frac{m}{\left[\left(m^2/a^2\right) + \left(n^2/b^2\right)\right]^2} \cdot \cos\frac{m\pi\xi}{a} \sin\frac{n\pi\eta}{b} \sin\frac{m\pi x}{a} \sin\frac{n\pi y}{b} \qquad (1.3.3.1)$$

with:[15]

$$D = Eh^3/[12(1-v^2)] \qquad (1.3.3.2)$$

---

[13] Szilard, R., Theories and Applications of Plate Analysis: Classical, Numerical and Engineering Methods.

[14] Szilard, R., Theories and Applications of Plate Analysis: Classical, Numerical and Engineering Methods.

[15] Szilard, R., Theories and Applications of Plate Analysis: Classical, Numerical and Engineering Methods.

2.1. Loading-Protocol

An object of this research is to diagnose the resistance of cold formed steel (CFS) connections under cyclic loading compared to connections under monotonic loading. An earthquake can be seen as such a cyclic event. The prediction of the strength, deformation capacity, and energy dissipation of a cold-formed steel member at a seismic event depends on how accurately the testing replicates an unknown future earthquake.[16] The influences of the strength, length and intensity of such an earthquake are endless. The type of connection, the place and the direction of the installation and dynamic properties of the system are only a few influences for it. Therefore the development of the loading-protocol should be considered more as an abstract model of an earthquake.

The developed loading protocol is based on the FEMA 461 quasi-static seismic protocol. Every two cycles the amplitude of the cycles increases. After six cycles the predicted capacity for the connection, calculated with the AISI S100, will be reached in accordance to that protocol. The change of the amplitude increases with a factor of 1.4 relative to the previous deformation step up to the 20th cycle. From this point on, the displacement changes linear.
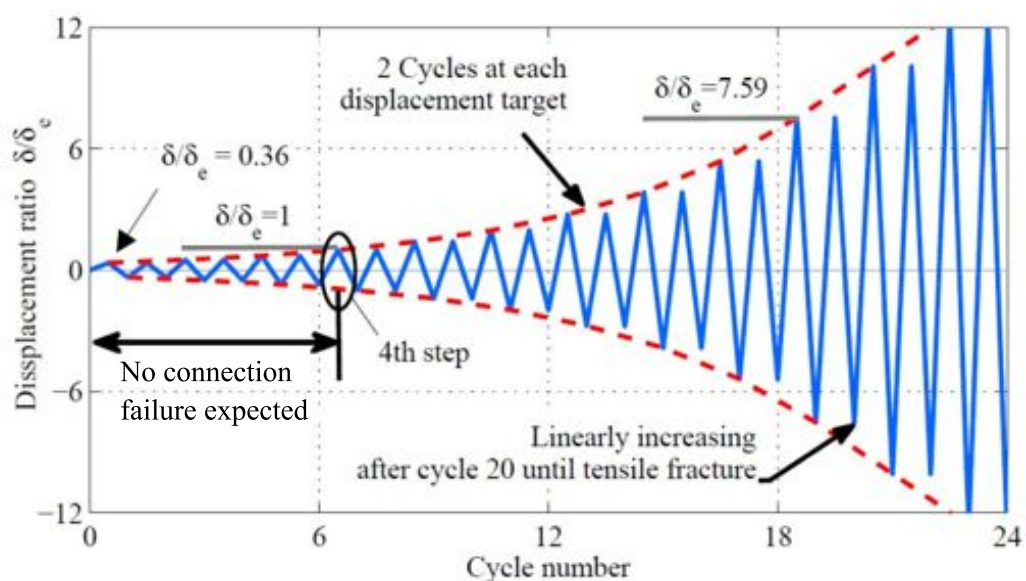
Picture 2.1.1. – Loading Protocol

---

[16] Padilla, D., Cyclic Energy Dissipation of Cold-Formed Steel Studs - Experiencing Euler Buckling.

Picture 2.1.1 shows graphically the correlation of displacement and cycle number. The variable δ_e is the deformation relating to the predicted capacity. The variable δ is the deformation relating to a variable point.

The test-rate for the protocol can be observed as a compromise between the total test time and producing data points. The cameras restrict the recording of the pictures of the non-contact measurement. The test time per cycle should last at least 16 seconds per cycle, to record enough pictures for the evaluation. To reduce the total-test-time the test-rate will be changed 4 times while testing. Table 2.2.1 gives an overview of the different test-rates of the cyclic tests.

Cycles	Test-Rate [in./s]
1-6	0.001
6-10	0.004
10-20	0.008
21-end	0.016

Table 2.2.1. – Test-Rates for the Loading-Protocol

2.2. Types of Connection

In this research, two types of connections were tested. Picture 2.2.a shows the tested web-to-web connection, which is typically used to create stronger columns or larger beams. The other type of connection is a web-to-flange connection, which is shown in picture 2.2.b. This connection is common used for column-beam connections.

There were also three different thicknesses tested. The thinnest ones are 0.88 mm (0.0346 in.) thick. The next have a thickness of 1.15 mm (0.0451in.) and the thickest have a thickness of 2.58mm (0.1017 in.). The combination of the thicknesses was as followed:

- 0.88 mm to 0.88 mm (#33)
- 1.15 mm to 1.15 mm (#44)
- 2.58 mm to 0.88 mm (#103)

The depth of the members for all tests is 152.4 mm (6 in.) with a flange length of 41.275 mm (1.625 in.)[17].

In the following report the web-to-web connection is additionally labeled with WW and the web-to-flange connection with WF.

Picture 2.2.a. – web-to-web connection (WW)   Picture 2.2.b. – web-to-flange connection (WF)

2.3. Test Set-Up and procedure

The heart of the test set-up is the MTS Insight with an electromechanical system. This machine is a twin column floor standing model and is able to bring on a load of 150 kN. The moving and force generating component of this system for setting up and testing is the crosshead.[18] It can be moved vertically and collects the data like displacement and load. An aluminum bracket is attached to the crosshead to connect the crosshead with the steel members. To connect the bottom stud to the MTS, there is also an aluminum bracket. To be more flexible while installing, the bottom bracket is connected to a rail and can be moved horizontally. Picture 2.3.1 shows a picture of the whole test set-up. The top bracket is connected to the crosshead by a rod. The top test member is clamped and fixed by three 3/8" bolts. The bottom bracket consists of an aluminum plate on which, in case of web-to-web tests, the test member is connected with four 3/8" bolts. For the web-to-flange connection only two 3/8" bolts were used. To increase the stiffness and to decrease the deformation of the aluminum plate, a second aluminum plate is attached orthogonal to the vertical and bottom plate.

---

[17] Clarkdietrich.com

[18] MTS, Manual – Using TestWorks4.

The procedure to install the test members is as follows. The test members were drilled before the test to reduce a pre-load because of unwanted deformation while installing. After measuring the thickness of the studs, which is necessary to calculate the predicted strength, the bottom members were attached to the bottom bracket. The bolts on the slit were loose to reduce again a possible pre-load. At the second step the top member, who is also pre-drilled, will be attached to the bracket. After this was done, the bottom bracket can be adjusted and fixed. To consider possible load because of screwing the members together, at this point, the load cell has to be zeroed. Now the screw was set in position. The targets must be attached on the screw and the members to prepare the non-contact measurement. This happens by using wood sticks and hot glue.

The last step of preparing the test is to set up the cameras. There is one camera for the non-contact measuring of the screws and a second camera for the measurement of the relative displacement of the studs.
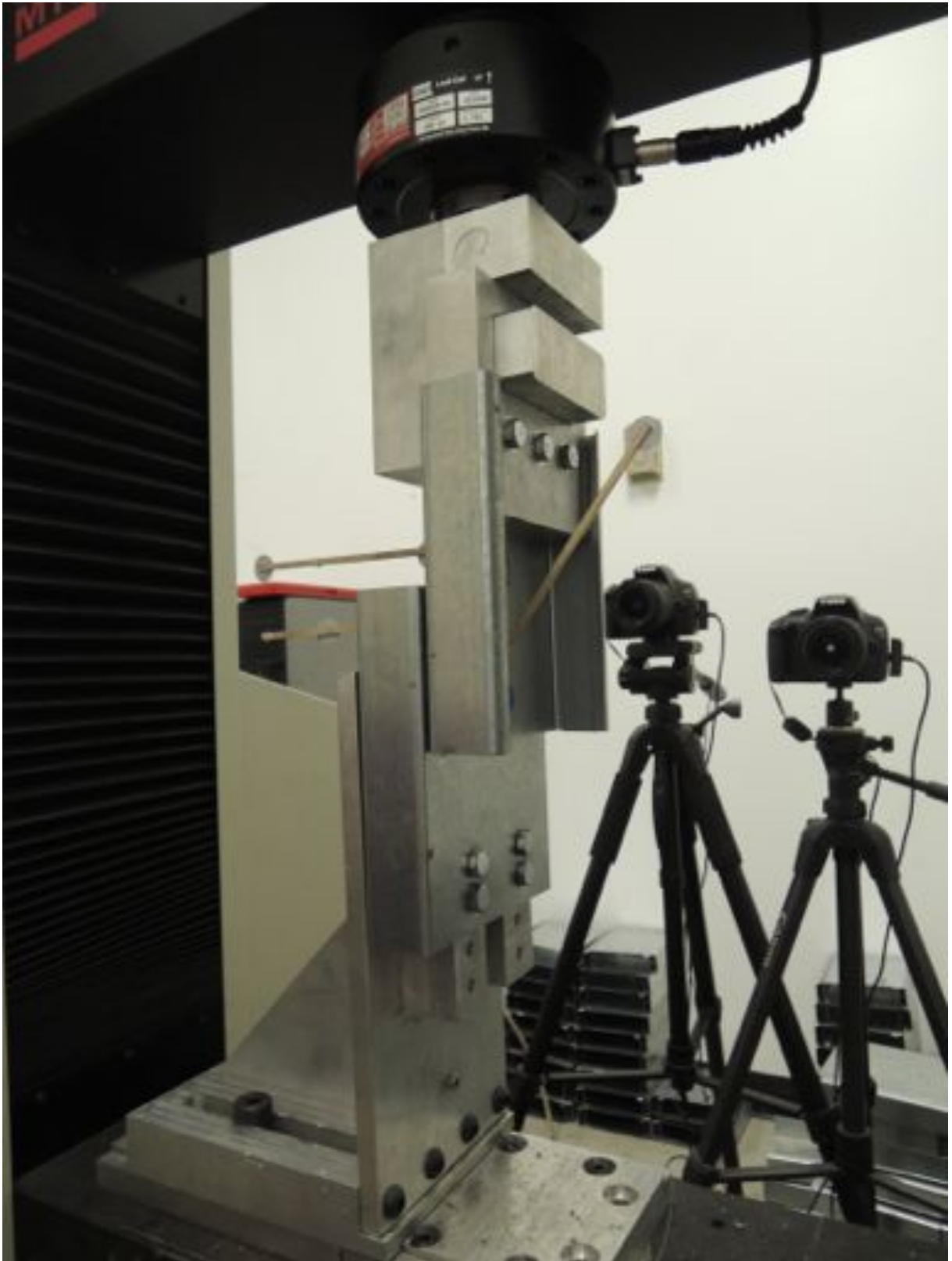
Picture 2.3.1 – The test setup

3. Measuring

3.1. Measuring Systems

The measuring unit of the MTS Insight is the crosshead. Combined with software and additional tools, a wide range of measurements can be done. For this test setup it is necessary to determine the connection load and also the relative ply displacement. The load and the ply displacement can be measured with the crosshead of the MTS Insight, where the resolution of the movement is about 0.001 mm.

An additional measuring system is the noncontact measuring. The noncontact measuring observes the screw and is used to get a better understanding of the different failure modes of cold form steel constructions. Main object of the noncontact measuring is to record the movement of the screw. As common measuring instruments are hard to attach to a screw, it was necessary to develop a new measuring method, which could record the vertical displacement as well as the rotation of the screw. This new method is based on a series of pictures, which were analyzed with Matlab software. The following chapters give a small introduction about the collection of the data and how to use the software.

3.2. Collecting the Data

As mentioned above, main object of the noncontact measurement is to record the movement of the screw, which means the vertical movement as well as the rotation of the screw. Both movements are important to know to get a better knowledge about failures like bearing and tilting.

Picture 3.2.1.1. – Collecting the data

Two Canon EOS 450D digital cameras conducted the collecting of the data. These cameras were connected to a computer where the cameras were synchronized and the pictures were stored. Picture 3.2.1.1 shows the setup with the used cameras. Next to the measuring of the movement of the screw is another measuring on the studs (left side of the picture). This second measuring can be used as a verification of the measuring of the crosshead and provides a more detailed view of the movement of the studs because of bearing and tilting. As demonstrated on the right side of the picture a stick was attached to the head of the screw to measure the movement. This extension of the screw had two targets on it. These targets acted as reference points and could be analyzed by the software.

3.3. Analyze with Matlab

The Matlab program assists to show the behavior of the screw by providing a more detailed picture of the screw's movement. As there is no possibility to connect a sensor to the screw a non-contact method was developed and is described in the following.

The collected pictures of the test setup were evaluated in Matlab. Therefore a developed script, based on the Image Processing Toolbox of Matlab, locates the position of the targets on the images. These targets were filtered to minimize any influence of other objects in the pictures.
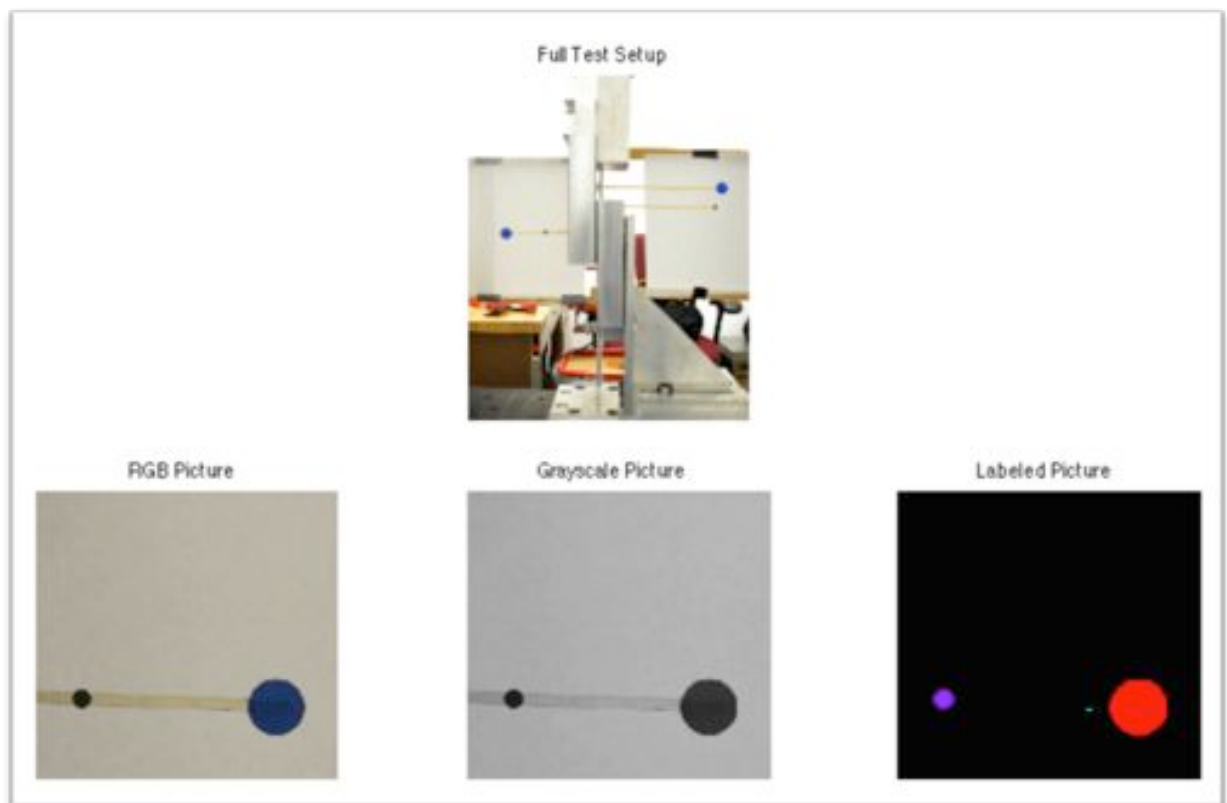

Picture 3.2.2.1. – Analyzing with Matlab

Picture 3.2.2.1 shows the process of the test setup. On top of this picture is the test setup as it is shown while testing. The first picture in the second line shows the picture like it comes from the camera. For a better contrast the pictures were converted to a grayscale picture. The following step labels all round objects on the picture, which means that the labeled objects

could be one of the targets, or a wrong pixel on the image. Finally a filter system chooses only the significant targets for the calculation.

In a following step, with the data of the located targets, the position and angle of the screw can be determined. The result is documented in picture 3.2.2.2. The three graphics within the picture show the angle and the displacement of the screw at it's the head and the movement of the target stick.
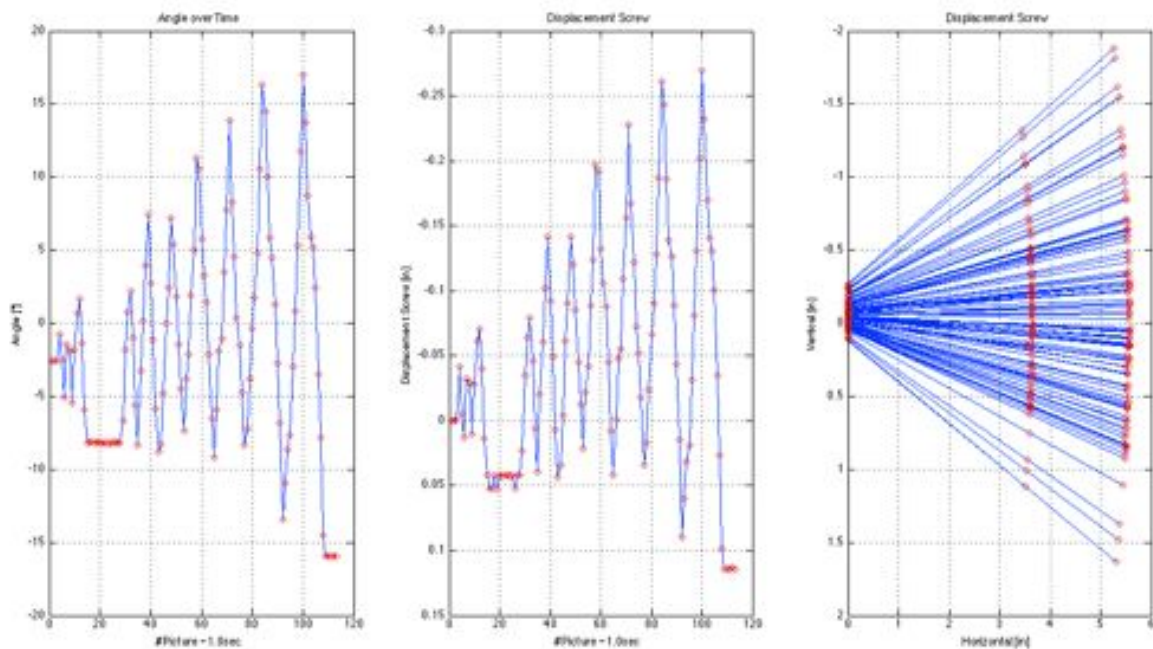
Picture 3.2.2.2. – Typical results from cyclic testing

3.4. Validation of the noncontact Measuring

For the validation of the noncontact measuring a small test series with ten calibration tests was conducted. The noncontact displacement was compared to the displacement of the MTS machine. As the coefficient of variation a value of 0.005 could be calculated.

MTS [mm]	Matlab [mm]
70.929500	70.66534
82.772504	83.49742
77.347826	76.47940
77.657452	77.26934
76.151994	75.90536
86.002114	86.15426
91.542108	91.15552
64.592200	64.37122
30.761686	30.67812
32.372300	32.30626

Table 3.2.3.1. – Results of the calibration

The length of the sticks and also the diameters of the balls on the sticks for the noncontact measuring were measured with an accuracy of 0.5 mm. The following accuracy of the noncontact measuring is enough for the evaluation of the Matlab results.

4. Head Study

4.1. Test Matrix

The Head Study investigates the difference of connections with different screw heads. The focus of this research is on the following four screws:

- Hex Washer Head
- Truss Head
- Flatpan Head
- Pancake Head

For the head study 48 tests were done. All of these were monotonic tests. Table 4.1.1 shows the test matrix for web-to-web and for-web-to flange connections with the number of conducted tests. There were at least two tests to be done to avoid any error in the measurements or in the screwed connection. If there was a big variation between the results of the same connection, more tests were conducted to verify the results.

Head Type / Stud Thickness [in.]	Hex Washer Head	Truss Head	Flatpan Head	Pancake Head
WW 0.0346 / 0.0346	2	2	2	2
WW 0.0451 / 0.0451	2	2	2	2
WW 0.1017 / 0.0346	2	2	2	2
WF 0.0346 / 0.0346	2	2	2	2
WF 0.0451 / 0.0451	2	2	2	2
WF 0.1017 / 0.0346	2	2	2	2

Table 4.1.1. – Test Matrix for Head Study

Table 4.1.2 gives a closer look to the details of the screws.

Screw Type		Model No.	Head Diameter [mm]	Threads per Inch	Code
	Hex Washer Head	X1S1016	10.5	16	HEX
	Truss Head		9.3	16	TRU
	Pancake Head	PCSD1S1016	10.3	16	PCH
	Flatpan Head	FPHSD34S1016	9.3	16	FPH

Table 4.1.2. - Overview of the screws

4.2. Tilting and Bearing Load Response Elastic / Theory Validation

The American Iron and Steel Institute Standard 100 knows seven different failure modes for steel-to-steel connections[19]. The seven failure modes are defined as follows:

- Tilting
- Bearing
- End Distance
- Shear in Screw
- Pull-Out
- Pull-Over
- Tension in Screw

[19] American Iron and Steel Institute, AISI STANDARD 100-2007-C.

To get an idea of the leading failure mode it is necessary to calculate the capacity of all the failure modes for all connections. With the AISI S100 the following capacities can be calculated:

Equation		Predicted Load [N]			Screw Type	Failure Mode
		# 33	#44	# 103		
E4.3.1	$P_{ns} = 4.2(t_2{}^3 \cdot d)^{1/2} \cdot F_{u2}$	1972.0	2934.7	1972.0	all	Tilting
	$P_{ns} = 2.7 \cdot t_1 \cdot d \cdot F_{u1}$	2970.7	3872.2	13230.0	all	Bearing
	$P_{ns} = 2.7 \cdot t_2 \cdot d \cdot F_{u2}$	2970.7	3872.2	2970.7		
E4.3.2	$P_{ns} = t \cdot e \cdot F_u$	34745.1	45289.2	34745.1	all	End Distance
E4.3.3	P_{ss}			8235.9	HEX	Shear in Screw
				8460.3	TRU	
				7652.4	PCH	
				7652.4	FPH	
E4.4.1	$P_{not} = 0.85 \cdot t_c \cdot d \cdot F_{u2}$	935.2	1219.0	935.2	all	Pull-Out
E4.4.2	$P_{nov} = 1.5 \cdot t_1 \cdot d'_w \cdot F_{u1}$	3596.1	4687.4	16015.3	HEX	Pull-Over
		3891.5	5072.4	17330.6	TRU	
		3800.2	4953.5	16924.4	PCH	
		3240.0	4223.2	14429.3	FPH	
E4.4.3	P_{ts}			12833.1	HEX	Tension in Screw
				9430.2	TRU	
				10586.8	PCH	
				9852.8	FPH	

Table 4.2.1. – List of the predicted load of different connections

In equation *E4.3.1 Connection Shear Limited by Tilting and Bearing* t_1 and t_2 are equivalent the thickness of the studs. t_1 is the thickness of the stud on the side of the head of the screw, t_2 the thickness of the stud on the other side. F_u means the ultimate stress for the steel. The ultimate

stress for a thickness of 0.0346 in. and 0.0451 in it is 25.5 kN/cm^2. For a thickness of 0.1017 in. it is 39.0 kN/cm^2.

The variable *d* means the diameter of the screw. For #10 screws it is 4.83 mm. The variable *e* in equation *E4.3.2 Connection Shear Limited by End Distance* means the shortest edge distance in load direction. The predicted loads for equation *E.4.3.3 Shear in Screws* are given by the manufacture and can be looked up in the product catalog. The equations from chapter *E4.4* refer to tension loaded connections. Therefore the typical failure modes are Pull-Out, Pull-Over and Tension in Screws. *E4.4.1* describes the failure through Pull-Out where t_c means the thickness t_2. For the calculation of the predicted load for Pull-Over, equation E4.4.2 uses d'_w which means the "Effective pull-over diameter [...]."[20] Like the predicted loads for Shearing in Screws, the loads of *E4.4.3 Tension in Screws* are also given by the manufacturer[21].

As presented in Table 4.2.1 the lowest predicted capacity is because of failure E4.4.1 Pull-Out. This failure mode describes a tension failure mode. The load direction of the test setup is orthogonal to the screw. Therefore a tension failure mode can't be the first failure mode. It follows, that the predicted load must be the next higher calculated capacity, which means, that E4.3.1 Tilting is the leading failure mode.

Picture 4.2.1 shows the typical behavior, which can be seen while testing. In the very beginning there is tilting. The load rises in a kind of linear way close to the maximum load. In the picture it was marked in blue. The green line presents the combination of tilting and bearing. Bearing can be seen as a plastically deformation on the studs.

[20] American Steel and Iron Institute, AISI STANDARD 100-2007.

[21] Strongtie.com.
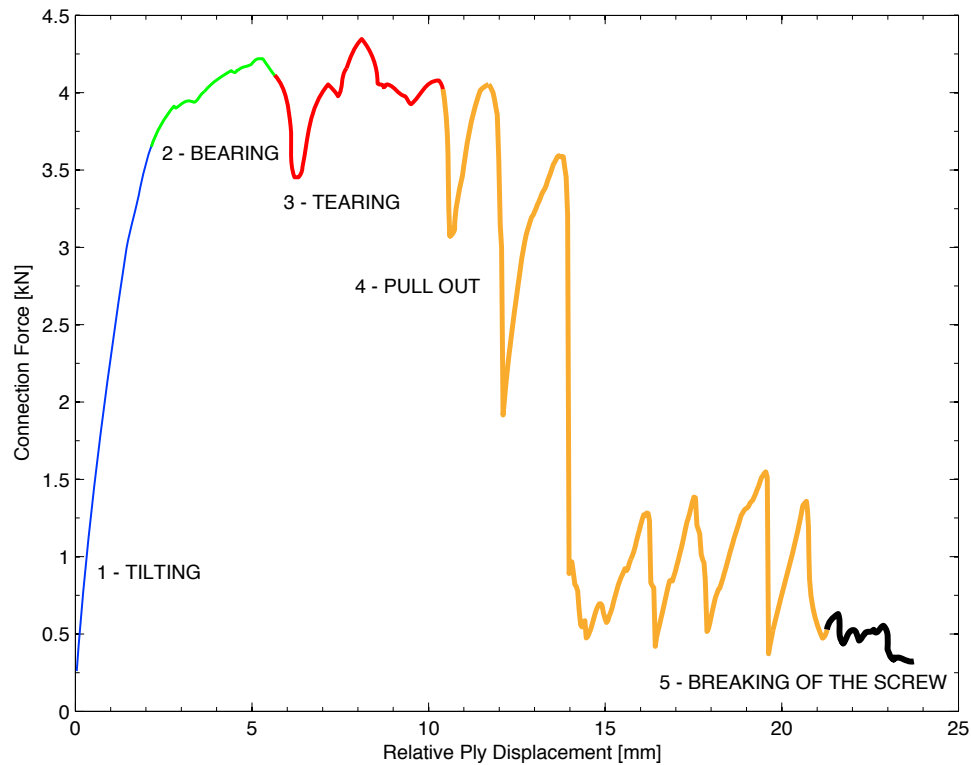
Picture 4.2.1. – Typical load-displacement behavior

Typical for bearing is the decline of the slope of the curve. The cross over from bearing to tearing is fluently. This part is marked in red. Tearing can be seen as an irregular increasing and decreasing of the load-displacement-curve. The following yellow part shows pull-out. After the rotation of the screw because of tilting is done, the screw has an additional load in form of tension. The different load drops show when a thread slips through the hole of the stud. The black line at the end of the curve shows the final failure mode when the screw fails.
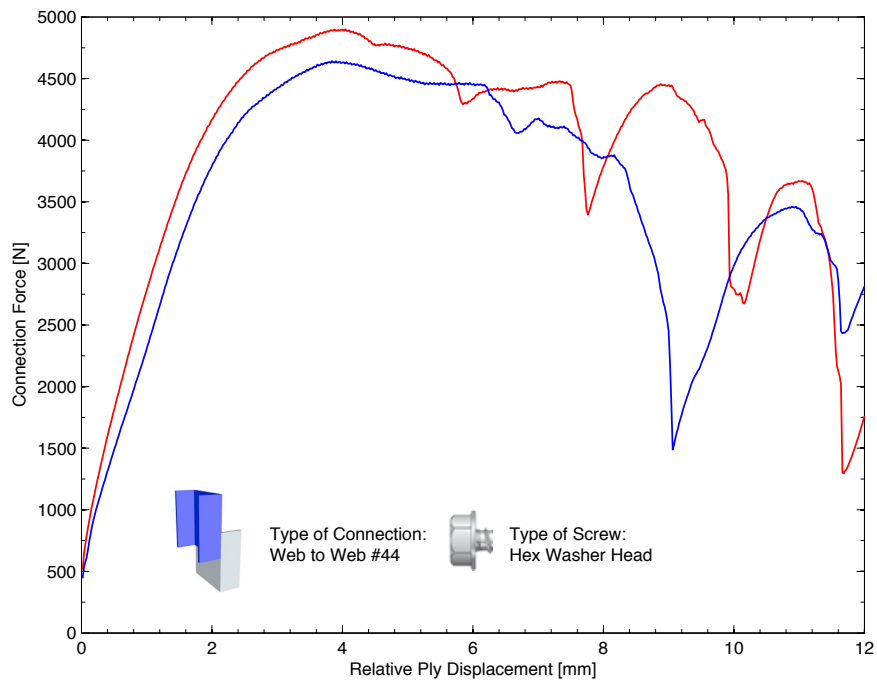
Picture 4.2.2 shows the load-displacement behavior of number 10 (#10) Hex Washer Head Screws in a #33 web-to-web connection. The behavior for both tests was the same. After the tests start, signs of tilting were seen until the head of the screw was pressed to the stud. After this point, there was no possibility for more tilting and tilting changed to bearing in both members.
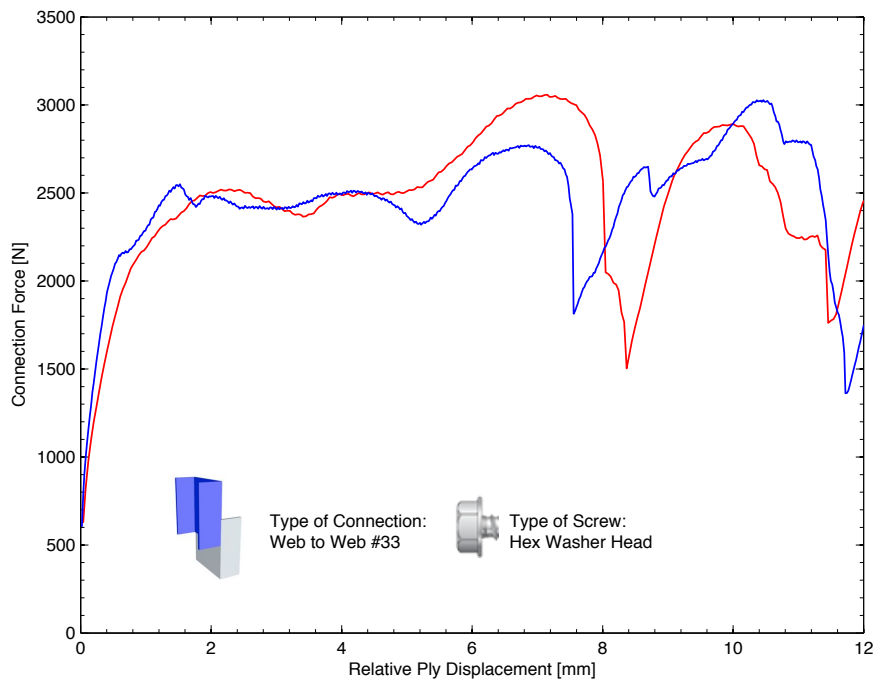
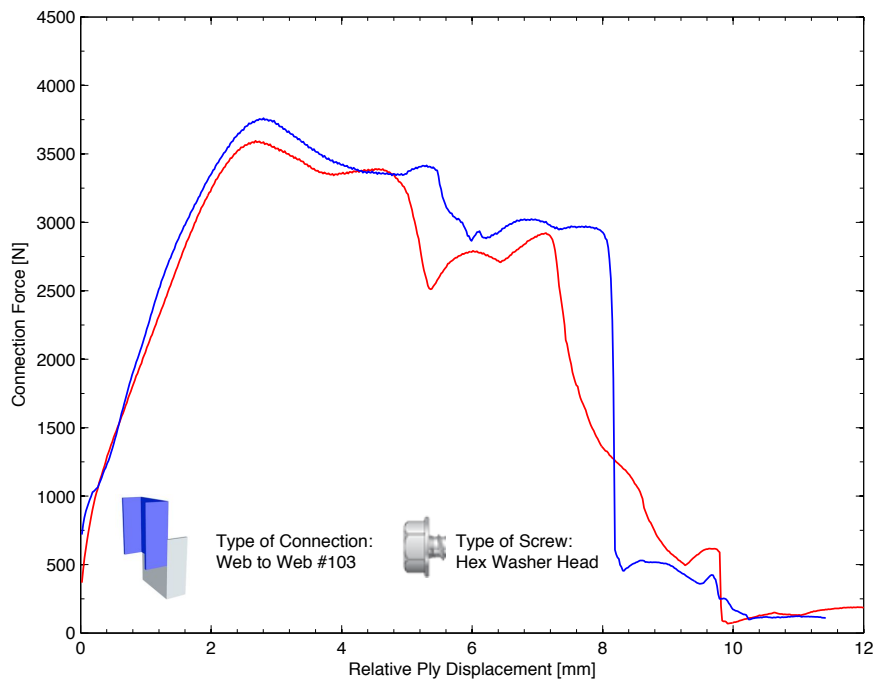Picture 4.2.2. – Load-Displacement behavior #10 HEX #33 WW

In Picture 4.2.2 bearing can be seen at a displacement of about 2 mm, where the slope of the curves decreases. While the load is constant and the displacement increases, a separation of the sections is seen. When the load drops after the peaks, it illustrates some pull out. At the same time there is a lot of tearing in the lower member when the thread tries to slip through the hole. It seems, that when the thread grabs again, also the load increases again. These increasing and dropping of the load continues until the whole screw pulled out.

Picture 4.2.3 also presents web-to-web connections with Hex Washer Head Screws. In this case the thickness of the members #44. In the beginning of the test, the load displacement behavior seems to be linear and shows signs of tilting. After the head of the screw touched the member, the curve flattens and shows some bearing. However, compared to the #33 tests, there is less bearing in the members. At a displacement between six and seven millimeters, pull out starts. In contrast to the #33 connection tests, while testing #44 connections these screws break before they slip completely out.
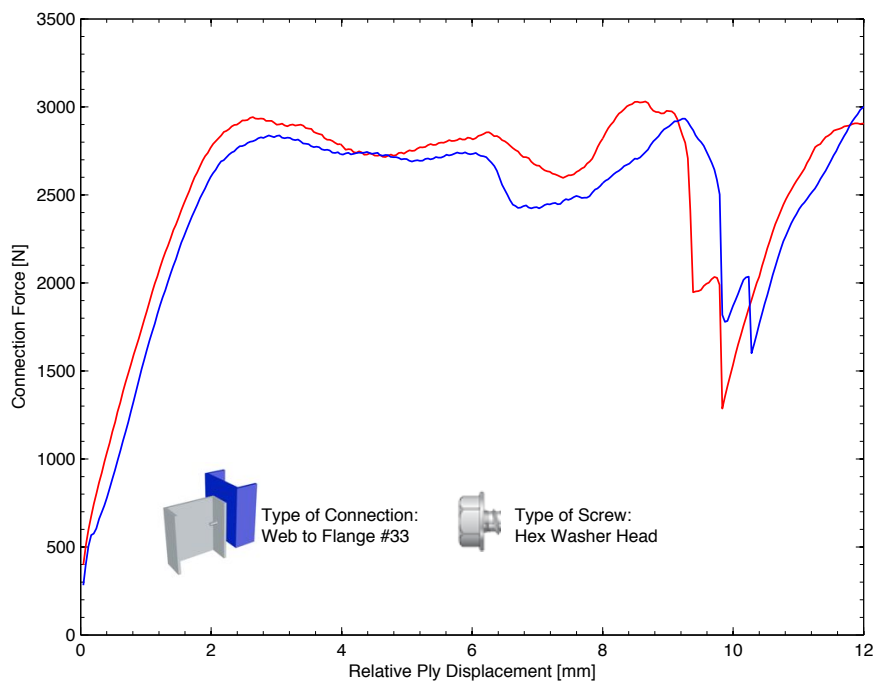
Picture 4.2.3. – Load-Displacement behavior #10 HEX #44 WW

Picture 4.2.4 shows the curves of #103 web-to-web tests with Hex Washer Heads. The tests show no indication for tilting and start directly with bearing. Compared to the #33 and #44 tests, there is a lot of bearing only appearing in the thinner studs. There can also be inspected a lot of separation between the studs, where only the thinner stud is bending to the back. During time of separation, there is some noisy pull out of single threads. This can be seen in the plot, when the load drops. All tests in this series end with a break of the screw.
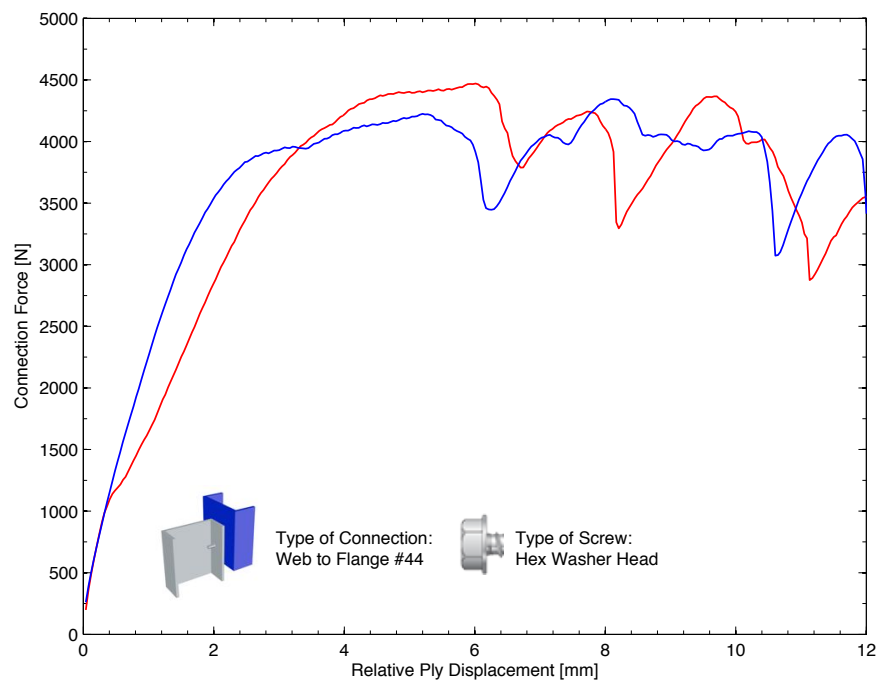
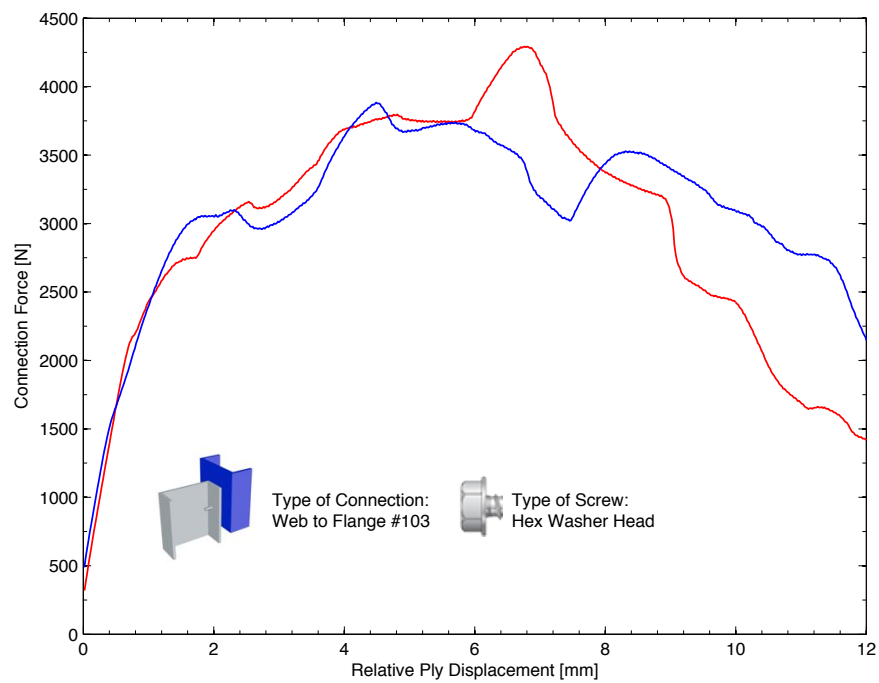Picture 4.2.4. – Load-Displacement behavior #10 HEX #103 WW

Picture 4.2.5 to picture 4.2.7 show the test series for the web to flange connection. A similar behavior was observed and will be discussed in the following chapters.

Picture 4.2.5. – Load-Displacement behavior #10 HEX #33 WF

Picture 4.2.6. – Load-Displacement behavior #10 HEX #44 WF

Picture 4.2.7. – Load-Displacement behavior #10 HEX #103 WF

4.3. Interpretation of the Head Study

4.3.1. Connection Stiffness

As mentioned in chapter 1.3.3, the idea behind the Plate Theory is to achieve a reference displacement. Therefore it is necessary to verify the results of the Matlab script with the results of the plate theory from chapter 1.3.3.

As the Matlab program gives only a rotation of the plates, the equation 1.3.3.1 must be transformed to the rotation and adapted to the center of the plate.

The rotation can be seen as the derivative of the displacement. For this case, the boundary conditions were set as follows:

- $a = b$ *(square plate)*
- $\xi = a/2$
- $\eta = a/2$
- $x = a/2$
- $y = a/2$

After differentiating the equation and using the boundary conditions, the new equation for the rotation is as follows:

$$w' = \frac{4M}{\pi^3 a^3 D} \sum_m \sum_n \frac{m}{\left[\left(m^2/a^2\right)+\left(n^2/b^2\right)\right]^2} \cdot \cos^2\frac{m\pi}{2}\sin^2\frac{n\pi}{2}\frac{m\pi}{a} \qquad (4.3.1.1)$$

The variable t affects this equation since it is based on the thickness of the connection. Here it is interesting to see, whether the connection behaves more as one thick plate, rather than only one of these plates.

Picture 4.3.1.1 illustrates a comparison of the results of the plate theory with the results of one of the conducted tests. The results of the test are representative. The magenta and red lines demonstrate the behavior of the calculated plate theory. The difference of the slope is

attributed to variable t. For the magenta line, t was set to $t = t_1 + t_2$ which means, that both plates work together as one plate. For the red line, t was set to $t = t_2$, meaning that only one plate of the connection has an influence on the behavior of the system.

The blue line is made of data from a conducted test. The angle comes from the noncontact measuring and the moment is calculated with the load of the MTS.
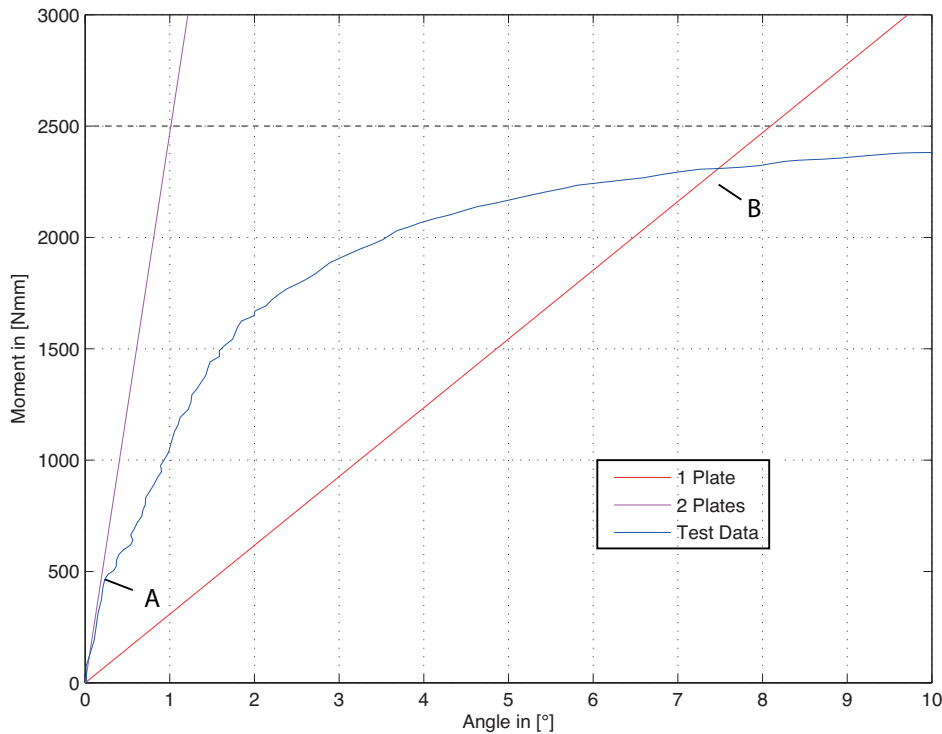
Picture 4.3.1.1. – Comparison Plate Theory – Test Data

The comparison of the plate theory and the measured data shows a non-linear behavior of the measured data (blue), whereat the plate theory (red and magenta) reflect a linear elastic behavior. In the beginning, when the test data shows a nearly linear behavior, the behavior of the test data is similar to the behavior of the two plates system. At a moment of about 500 *Nmm*, the separation of the plate theory and of the measured data starts (A). The curve grows more and more non-linear. The predicted moment with a load $P_n = 2,941\ N$ is about $M_n \approx 2,500\ Nmm$. This point is close to the point where the test data cross the plate theory with one plate (B).

It can be summarized that in the beginning, when the deformation and load is small (representing elastic behavior), a nearly linear behavior of the test data was determined. The

test data is close to the results of the plate theory considering a thickness of two plates. The equation for the plate theory is valid for an elastic behavior of the steel. For this part, the test results are close to the plate theory with $t = t_1 + t_2$. The point of failure is in a part of plastically behavior of the steel. As it can be seen in the picture this point of failure is also close to the plate theory with $t = t_2$.

For the loading protocol of the cyclic test, the plate theory with a thickness of $t = t_2$ is recommended. In this case the calculated displacement is nearly the same like the displacement of the tests at P_n.

## 4.3.2. Influence of the Screw Type

The influence of the screw type is one of the main objects in this research. As it can be seen in table 4.1.2, four different screw types were tested. Comparing all four screws, it is obvious that the head diameter of the Truss Head and the Flatpan Head screws are the same. The screw head of the Hex Washer Head and the Pancake Head are nearly the same. Therefore it can be assumed that these two pairs show a similar behavior.

Another interesting point in regard to the screws is the lower surface of their head. While the bottom side of the Hex Washer Head and the Pancake Head is flat, the bottom side of the Flatpan Head shows a ribbing. In contrast, the bottom side of the Pancake Head shows a thickening on the shaft (see table 4.1.2).
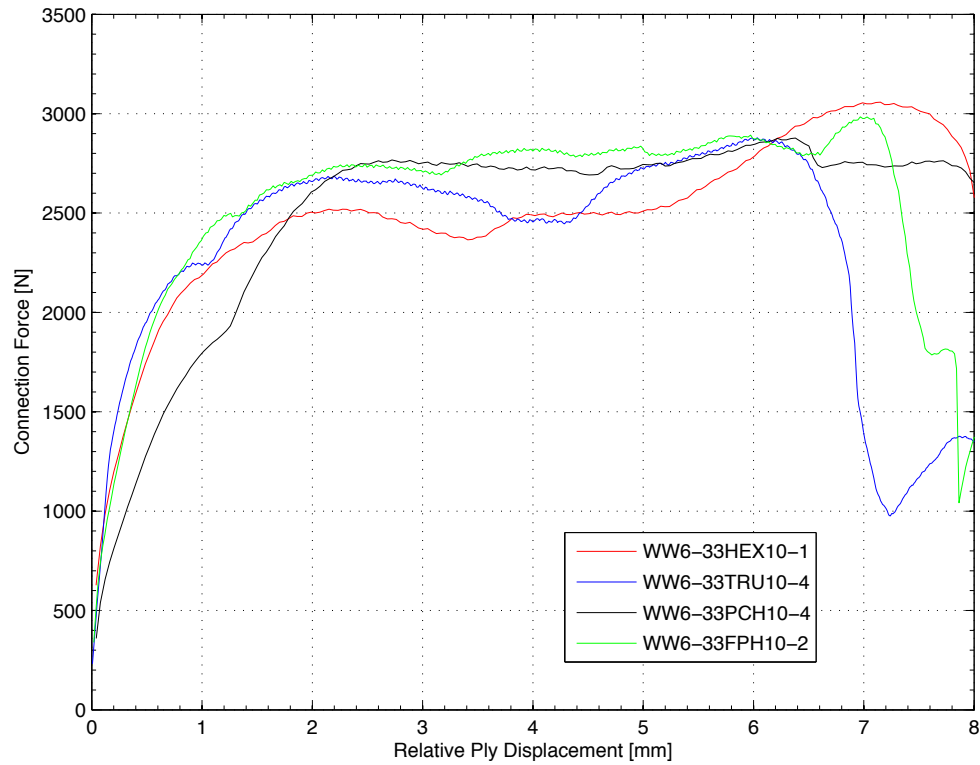
Picture 4.3.2.1. – Comparison of different head types

Picture 4.3.2.1 shows the comparison of the load-displacement behavior of different head types. The curves in the plot are representative for each type of screw. It is demonstrated, that the stiffness of the Hex Washer Head, the Truss Head and the Flatpan Head is nearly the same. Only the Pancake Head shows a lower stiffness. This suggests, that there is a connection between the lower stiffness of this type of screw and of the thickening of the shaft. In addition the maximum load for all the connections is approximately *2,800 N*. The predicted load for tilting is about *2,000 N*. After reaching 2,000 N, the stiffness of the connection changes to a non-linear trend. The predicted load for bearing is about *2,900 N*. This capacity is close to the load of *2,800 N,* where a plastically deformation starts.
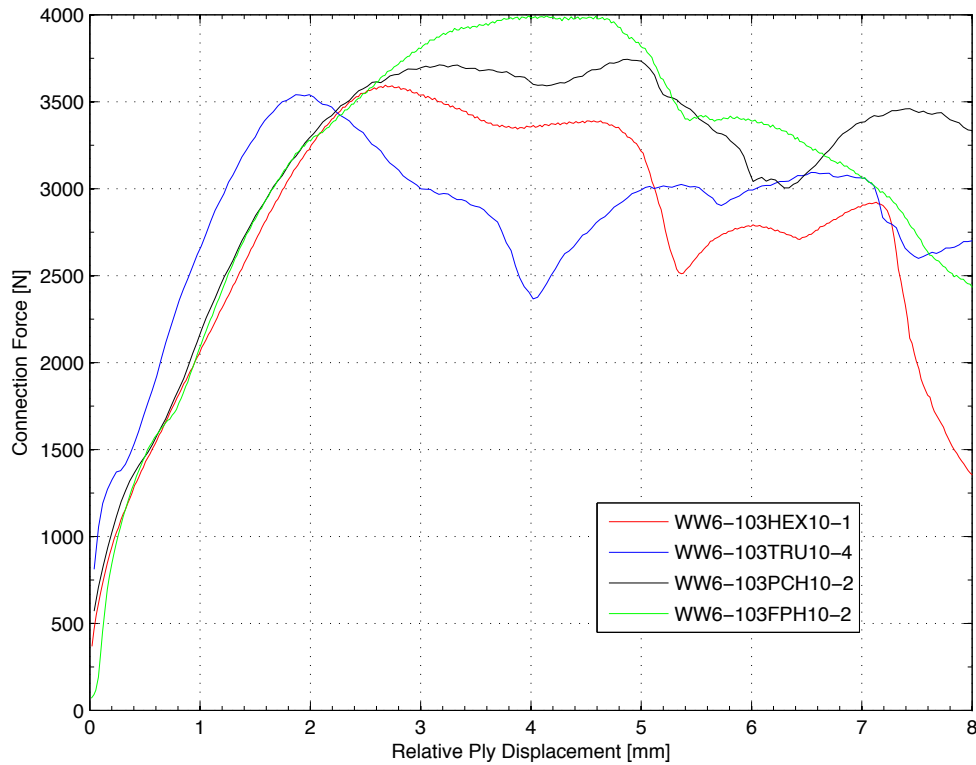
Picture 4.3.2.2. – Comparison of different head types for #103 connections

Another special case is the #103 connection. Picture 4.3.2.2 presents that all the screw types show the same stiffness. This characteristic will be discussed in chapter 4.3.3.

4.3.3. Influence of the Material Thickness

As mentioned in the chapter before, there is a difference between a #33 connection and a #103 connection even if the qualitative behavior of the different screw types seems to be the same. Therefore, the focus in this chapter is on the Hex Washer Head screws which can be transferred to the Truss Head, Pancake Head and Flatpan Head screws.

Table 4.3.3.1 shows the predicted load for different connections. It is remarkable, that the capacity of a #33 connection is the same like a #103 connection. The #44 connection, whose total thickness is smaller than the thickness of a #103 connection, has the highest capacity.

| Equation		Predicted Load [N]			Failure Mode
		# 33	#44	# 103	
E4.3.1	$P_{ns} = 4{,}2(t_2{}^3 \cdot d)^{1/2} \cdot F_{u2}$	1972,0	2934,7	1972,0	Tilting
	$P_{ns} = 2{,}7 \cdot t_1 \cdot d \cdot F_{u1}$	2970,7	3872,2	13230,0	Bearing
	$P_{ns} = 2{,}7 \cdot t_2 \cdot d \cdot F_{u2}$	2970,7	3872,2	2970,7	

Table 4.3.3.1. – Predicted Load different connections

This circumstance is based on the equations of the AISI S100, where the thinnest thickness is the determining factor. It is the same for a #33 and a #103 connection.

As suggested, the #44 connection has the highest capacity. The capacity of the #33 connection is the lowest. Between those the #103 connection can be found. The real capacity of the #33 connection is a bit lower than the real capacity. This is caused by lower thickness of the studs compared to the nominal thickness. The difference of the #103 connection results from a different failure mode.

As outlined in the table above, the first failure mode for #33 and #44 connections is tilting. From the beginning the curve followed a nearly linear trend up to the tilting capacity. After this point a clear non-linear trend began and bearing started.

The #103 connection showed a different behavior. Because of the thickness of the upper plate there was no possibility for a screw rotation. There was consequently no tilting. The deformation began with bearing and continued with tearing.
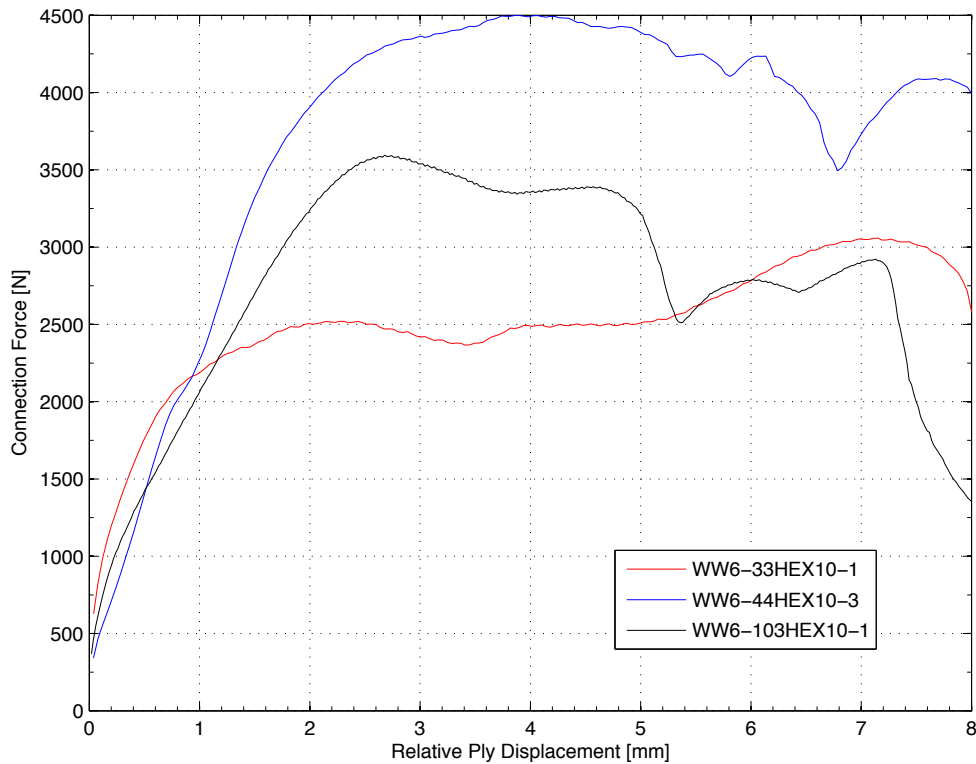
Picture 4.3.3.1. – Comparison of different thicknesses

The high capacity of the #103 connections as well as the increasing stiffness of the #33 connection at a relative ply displacement of about 6 mm is an indication for the characteristically steel hardening for cold-formed steel.

Transferring these results to the stiffness, it can be seen that the #33 and the #44 connections show a similar behavior. Their stiffness seems to be the same in the beginning and decreases at the point of the first failure mode.

The stiffness of the #103 connection is the lowest. This is mainly based on the fact that a screw rotation is missing. Compared to the other types of connections, the entire energy is dissipated through bearing in the thinner plate. While the #33 connections start with tilting and end with bearing, the #103 connections show only bearing. With the rotation of the screw the load in the screw changes from shearing force to normal force. The result is a combination of bearing and pull-out, whereat the thread of the screw tears the stud.

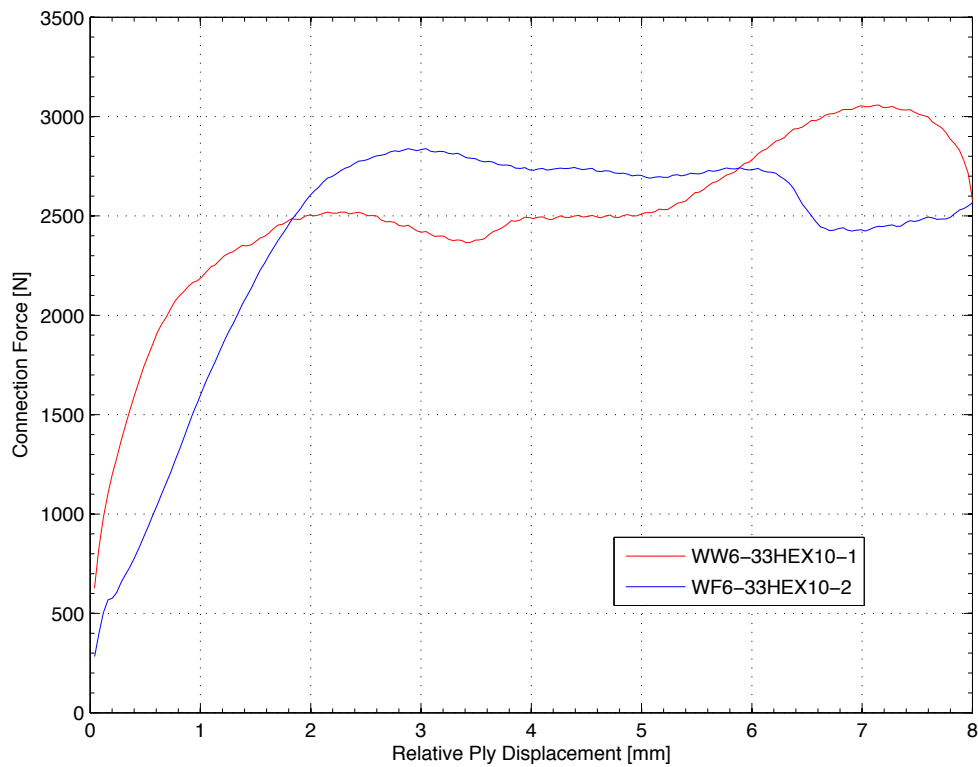### 4.3.4. Difference of Web-to-Web and Web-to-Flange Connection

Another important comparison is to compare between web-to-web and web-to-flange connection. This information supports the analyses of the influence of the boundary conditions on different connection types and to verify the boundary condition used for the plate theory.

The picture 4.3.4.1 shows this influence on the studs after removing them from the machine. The generated holes were big enough to remove the screw by hand. For testing, the screw was drilled from the upper to the lower stud.


Picture 4.3.4.1. – Area of influence screw

It can be seen, that the lower stud has a more significant damage. The yellow point can be used as a reference point. The diameter of this point is about 20mm. The area of influence is restricted to a small area next to the screw and the main damage is in the load direction.
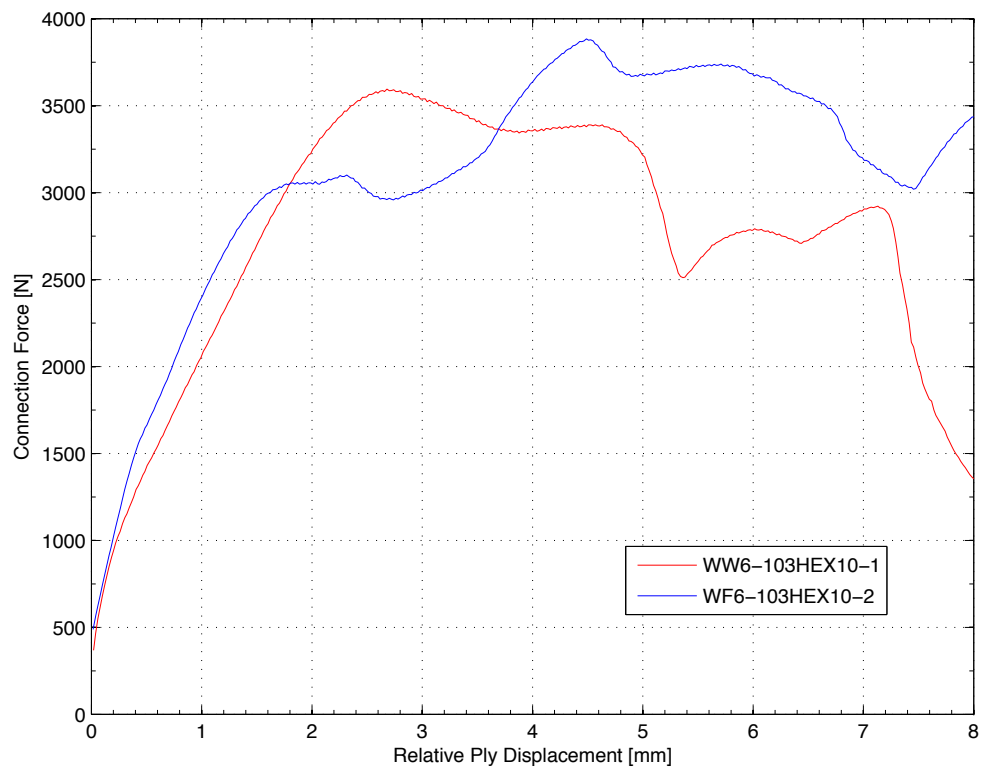
Picture 4.3.4.2. – Comparison of WW and WF #33 connections

Picture 4.3.4.2 to picture 4.3.4.4 shows a comparison of web-to-web and web-to-flange connections. It was observed that all pairs of connections have the same maximum capacity. Furthermore, the #44 and the #103 connection pairs show a similar stiffness. Only the #33 connections differ in the stiffness. As was determined, the stiffness of the web-to-flange connection is lower than the stiffness of the web-to-web connection.
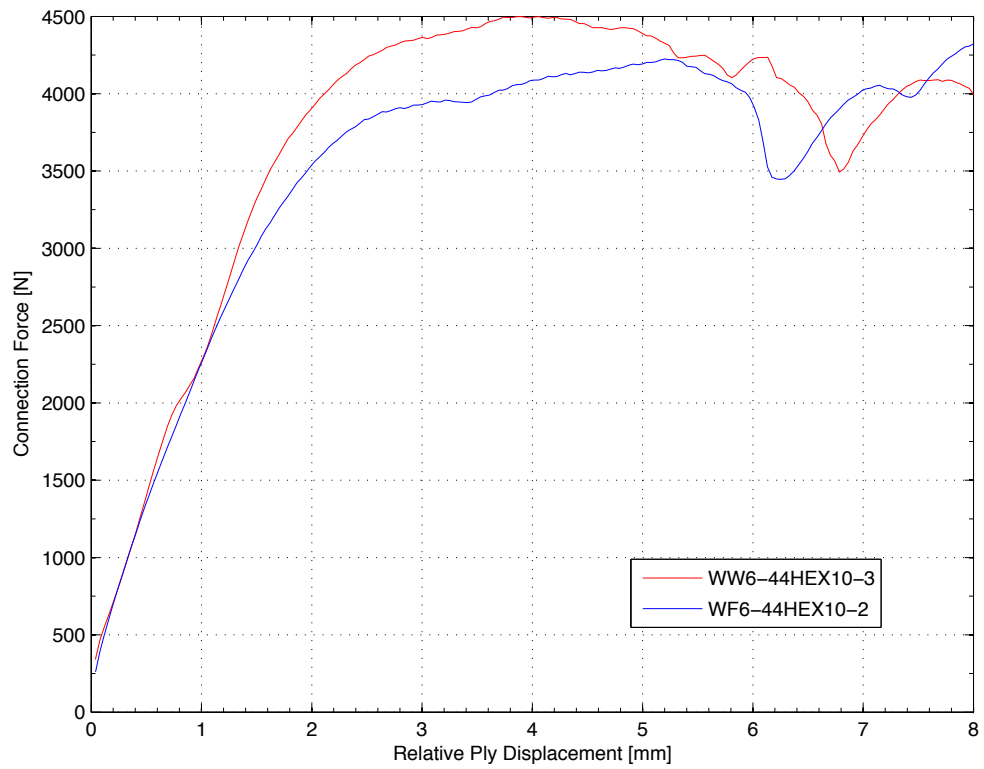
Picture 4.3.4.2. – Comparison of WW and WF #44 connections

Picture 4.3.4.3. – Comparison of WW and WF #103 connections

The reason for this difference is the gap between the studs, which can be seen in picture 4.3.4.5 a and b. In addition to the vertical displacement there is also a horizontal displacement between the studs. This horizontal displacement is different for web-to-web and web-to-flange connections.
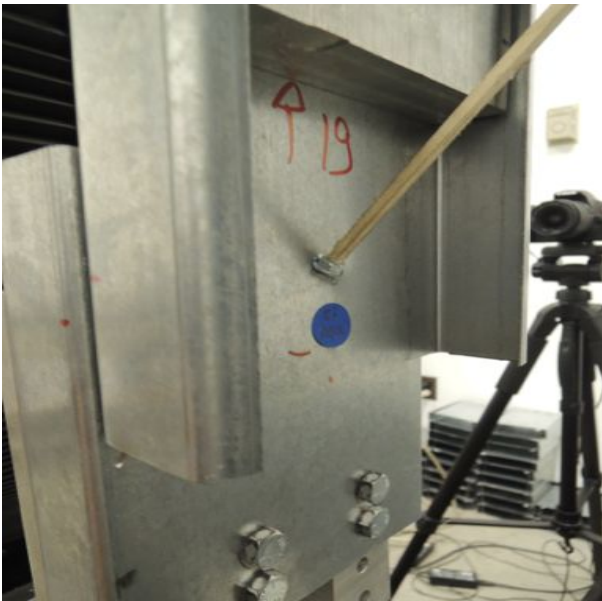
Picture 4.3.4.5.a. – Gap of a WW connection

Picture 4.3.4.5.b. – Gap of a WF connection

The stiffness of the members depends on their orientation. For the web-to-web connection, the stiffness for both members is the same. The deformation of both studs is the same because of a horizontal load.

For the web-to-flange connection, the stiffness of the lower member (in horizontal direction) is higher than the stiffness of the upper member because of the moment of inertia. It follows, that the horizontal deformation because of a horizontal load is different for the lower and upper stud. Because of a horizontal load there is a different deformation in the upper and lower stud.

The horizontal load is a result of the tilted screw and pull out.

It can be summarized, that the horizontal deformation was mainly in the upper stud, which gives a reason why there is no difference for the #44 and #103 connections. The stiffness of the upper stud for both connections is higher than the influence of the horizontal load. Because of the lower stiffness of the #33 connection, there is a deformation.

The screw's area of influence is concentrated to small area next to the screw and it is not influenced by the given boundary conditions.

5. Cyclic Testing

5.1. Test Matrix

After completion of the head study, the focus for the second part of the research is on the cyclic testing. Therefore only the influence of Hex Washer Head Screws on the studs was tested. Unlike during the head study, when to tests were conducted for each type of connection, three tests were arranged for each connection type during the second part of the research. Beside the configuration of web-to-web and web-to-flange, there is also a change of the screw's size. As a result, the common used sizes #8, #10 and #12, were tested.

Table 5.1.1 gives a more detailed look to the web-to-web and web-to-flange tests under monotonic loading while table 5.1.2 shows the test matrix for web-to-web and web-to-flange connections under cyclic loading.

As described in chapter 2.1 every test has its unique protocol, which is based on the thickness and the strength of the member. The strength of the members was measured with standard steel tension tests.

Screw Size / Stud Thickness [in.]	Hex Washer Head #8	Hex Washer Head #10	Hex Washer Head #12
WW 0.0346 / 0.0346	3	3	3
WW 0.0451 / 0.0451	3	3	3
WW 0.1017 / 0.0346	3	3	3
WF 0.0346 / 0.0346	3	3	3
WF 0.0451 / 0.0451	3	3	3
WF 0.1017 / 0.0346	3	3	3

Table 5.1.1. – Test Matrix Web-to-Web and Web-to-Flange monotonic Tests

Screw Size / Stud Thickness [in.]	Hex Washer Head #8	Hex Washer Head #10	Hex Washer Head #12
WW 0.0346 / 0.0346	3	3	3
WW 0.0451 / 0.0451	3	3	3
WW 0.1017 / 0.0346	3	3	3
WF 0.0346 / 0.0346	3	3	3
WF 0.0451 / 0.0451	3	3	3
WF 0.1017 / 0.0346	3	3	3

Table 5.1.2. – Test Matrix Web-to-Web and Web-to-Flange cyclic Tests

5.2. Test Results

At first view, it seems that there is an obvious difference between the monotonic and the cyclic tests. After a closer inspection to the test results, a similar behavior can be observed.

The failure modes of the AISI S100 were also found in the cyclic plots. As it was expected before, all the #33 and #44 tests started with tilting. Analog to the monotonic tests, the cyclic tests changed their behavior from tilting to bearing. As a result of the screw's rotation, the tension loaded screw showed some pull out. Because of the characteristic of the test type, each interval consisted of a push and a pull part. As long as the displacement of the connection increased, the screw connection was in tension with failure modes like tilting, bearing and pull out. After the maximum deformation of the interval was reached, the orientation of the deformation changed and decreased. At this point, the stress in the screw decreased. Passing the neutral position the same happened to the push side.

The deformation on the studs in the cyclic tests is more significant compared to the effects resulting from the monotonic tests. This is due to the loading and unloading process. The cause of increasing the holes in the studs was the start of tearing and pull out. At this point the thread of the screw stressed the connection. On the way back to the neutral position the

screw was pushed again in the hole and the thread worked again against the pull out.

It was interesting to see, that while testing, the screw unscrewed itself. This behavior started after the screw rotation was big enough to start pull out.

Picture 5.2.1 to picture 5.2.6 shows examples of this test series. All of the plots show #10 Hex Washer Head screws. As mentioned above, there is a high similarity between the behavior of the cyclic tests and the behavior of the monotonic test. The plots of the #103 connections confirm this. Instead of a discontinuous trend, influenced by pull out, the trend of the #103 tests is steady.
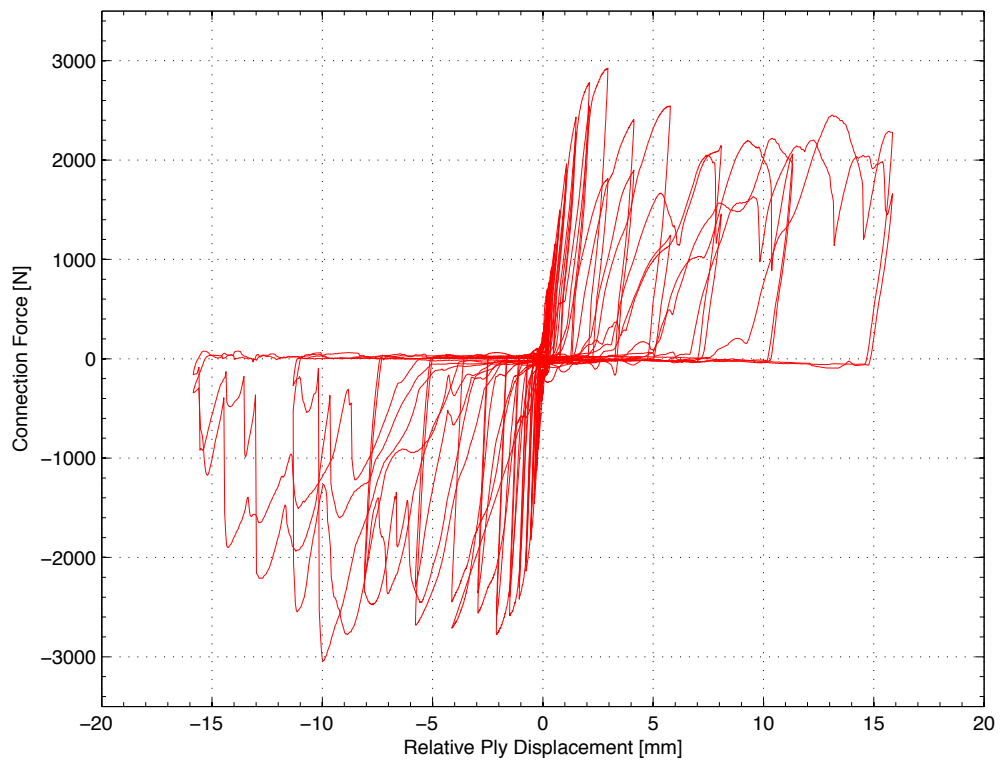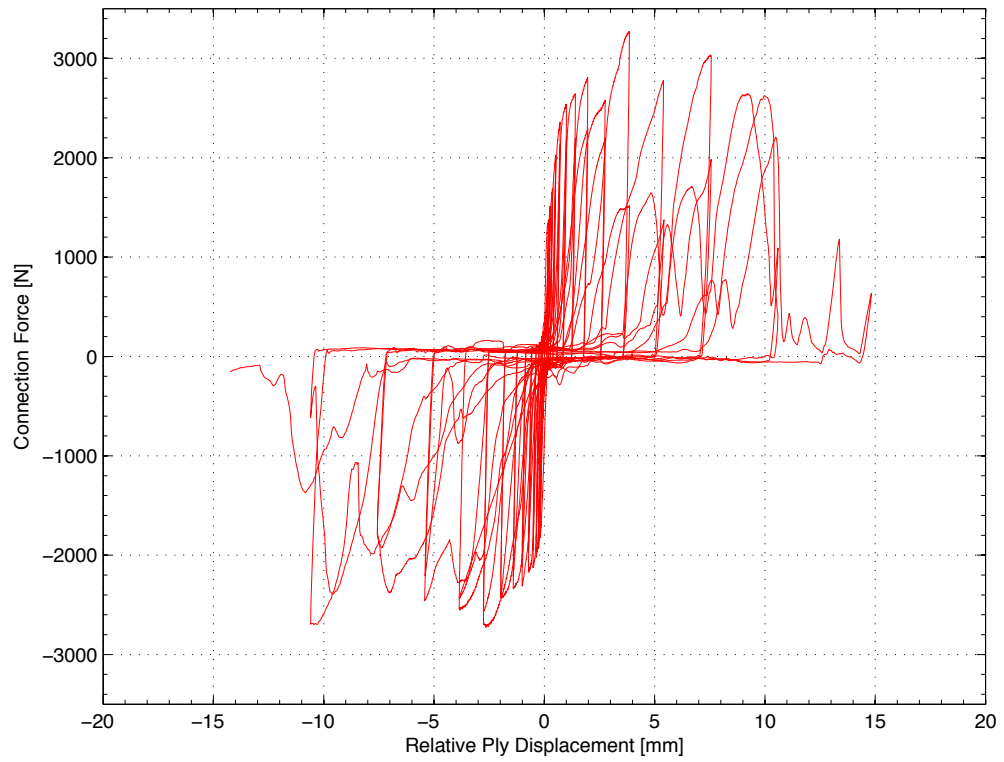

Picture 5.2.1. – Typical #33 cyclic web-to-web test
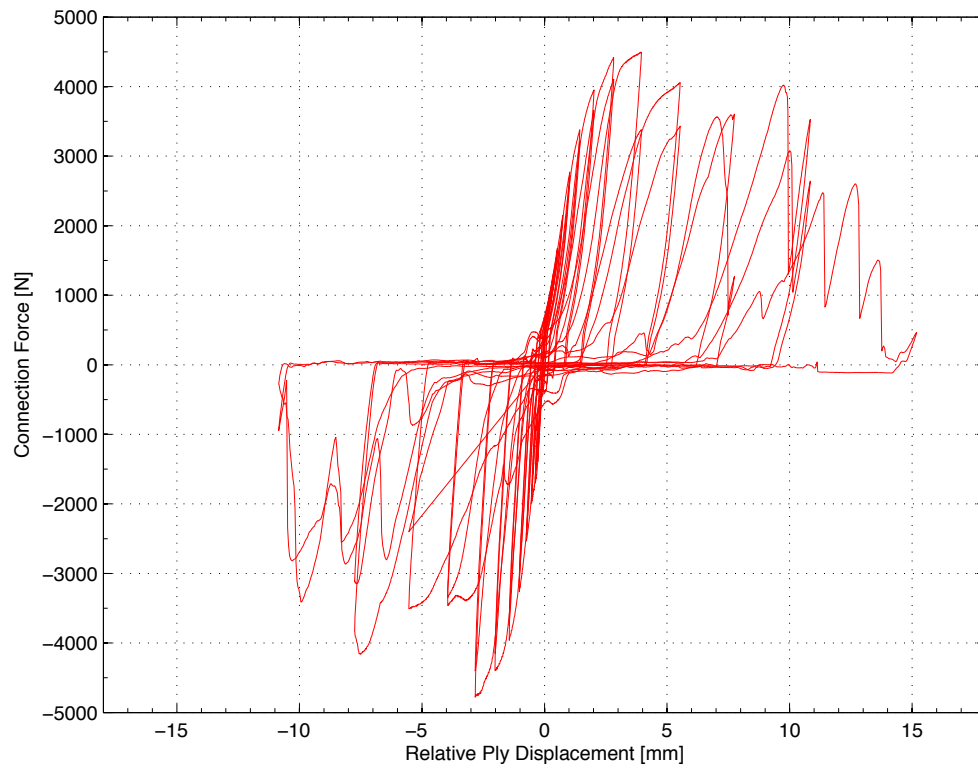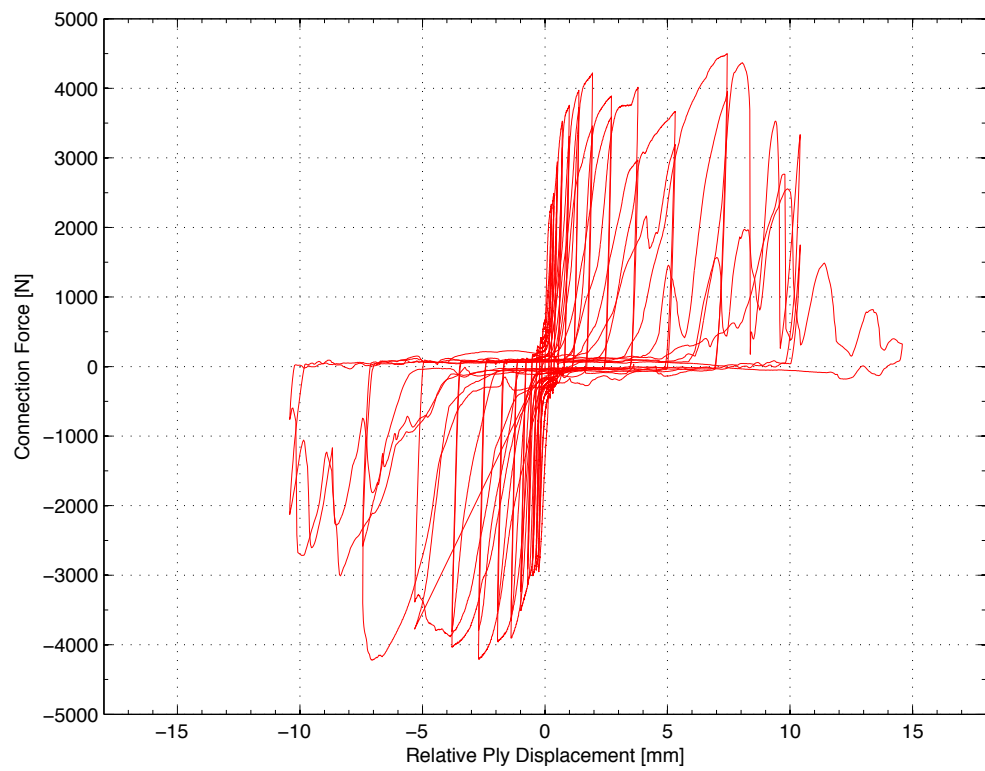
Picture 5.2.2. – Typical #44 cyclic web-to-web test
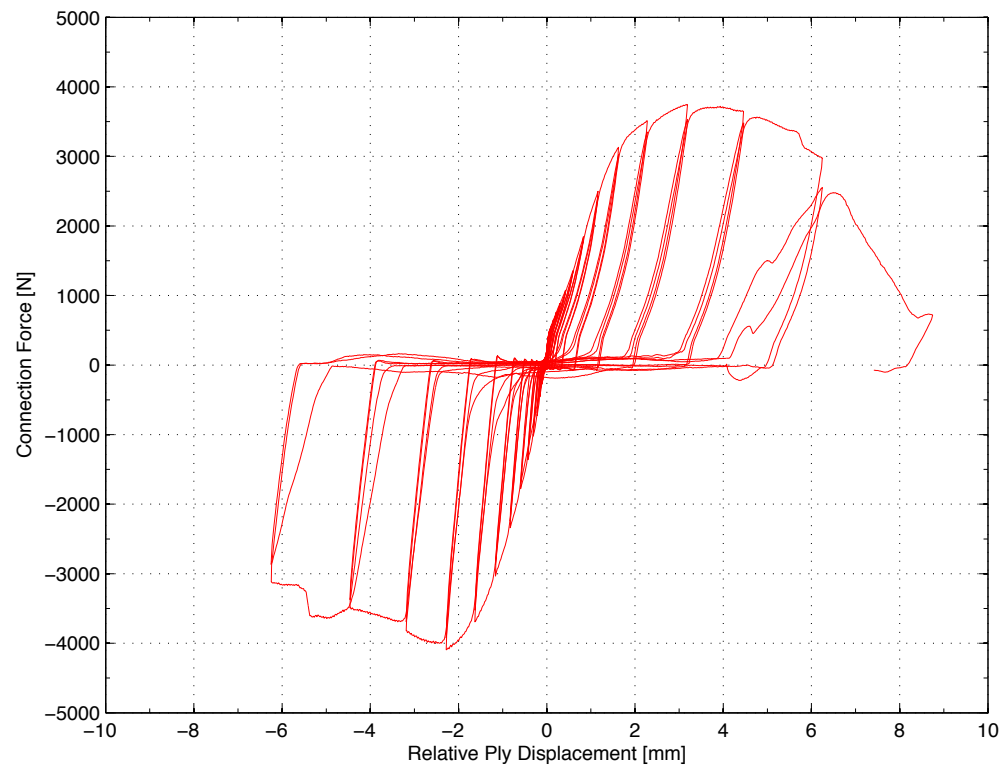
Picture 5.2.3. – Typical #103 cyclic web-to-web test

Picture 5.2.4. – Typical #33 cyclic web-to-flange test

Picture 5.2.5. – Typical #44 cyclic web-to-flange test
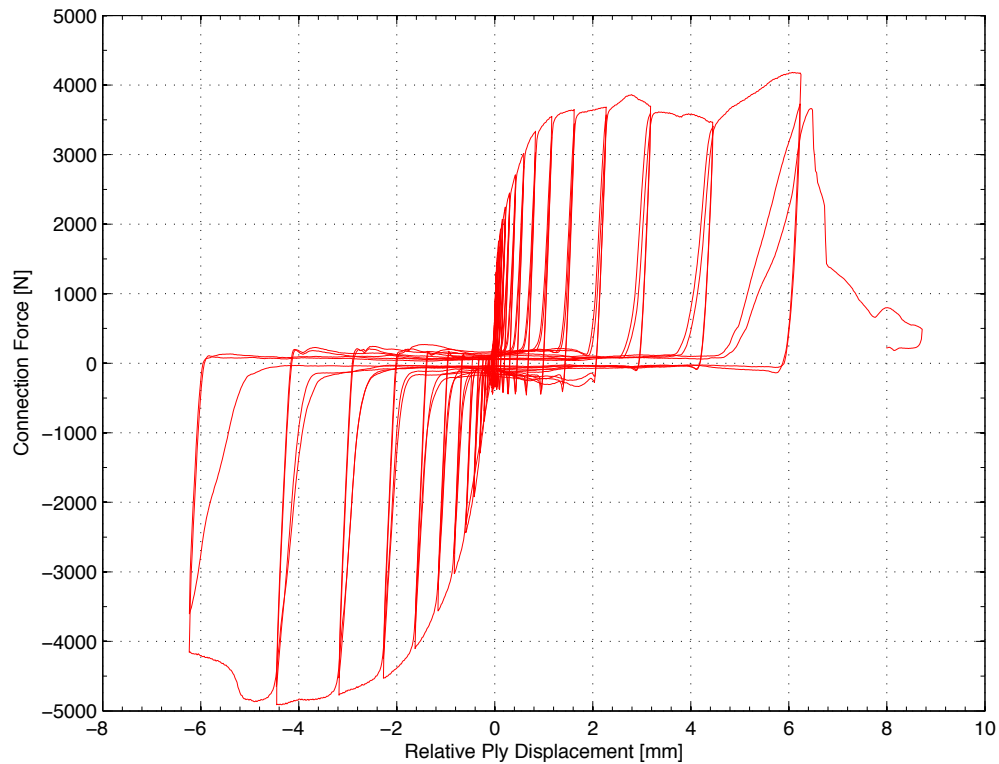
Picture 5.2.6. – Typical #103 cyclic web-to-flange test

5.3. Interpretation of the Cyclic Tests

5.3.1. Connection Stiffness

For monotonic testing, several push und pull tests were conducted. The results of the monotonic tests didn't show a difference between push and pull tests. Picture 5.3.1.1 illustrates a comparison of a push and a pull test. Stiffness, maximum load and failure modes of tests are the same for push and pull. The difference of cyclic test's push and pull side is remarkable.
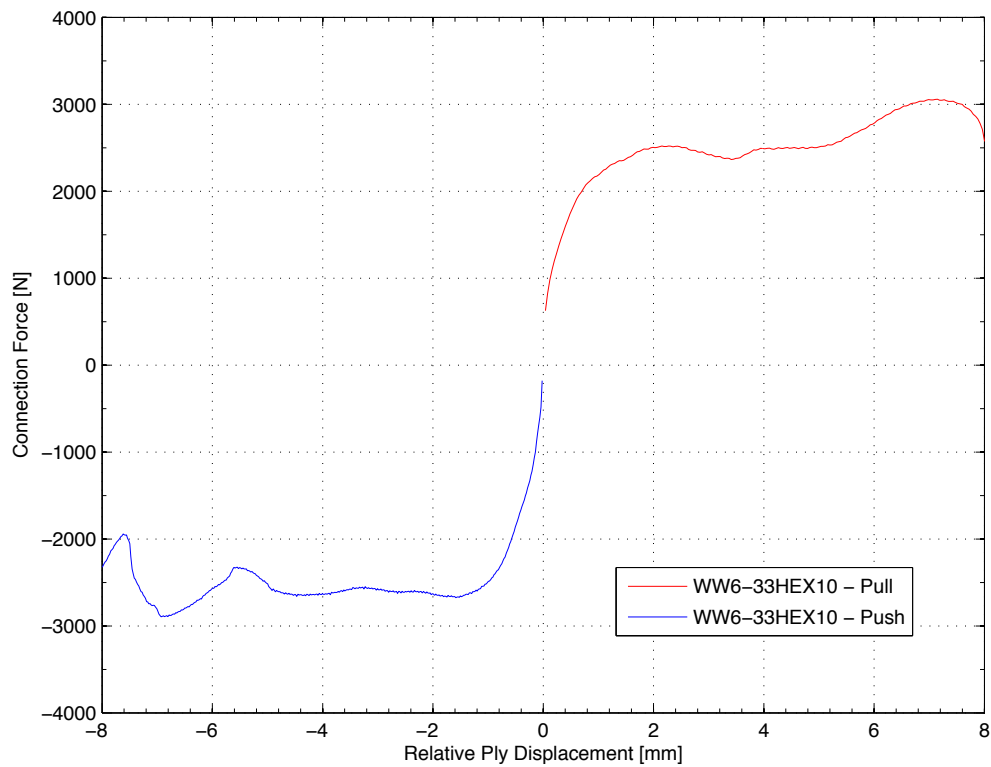
Picture 5.3.1.1. – Load displacement behavior WW6-33HEX 10 monotonic test

Picture 5.3.1.2 shows the load displacement behavior of cyclic tests of the same connection type like the monotonic test in picture 5.3.1.1. For a better clarity, the first six cycles are isolated plotted. The left column shows cycles of a new and bigger displacement, the right column shows the corresponding cycle with the same displacement.

It was found out, that for the same displacement, the push side shows the higher load. The trend on the pull side is flat and especially in the end of each cycle, the slope at the push side decreases.

This effect is different for all types of connections. While there is a big difference of the push and pull side for #33 tests, the behavior of #103 tests are symmetric. This means, that a less stiff connection has a bigger influence on pushing and pulling than a stiffer connection like a #103 connection.
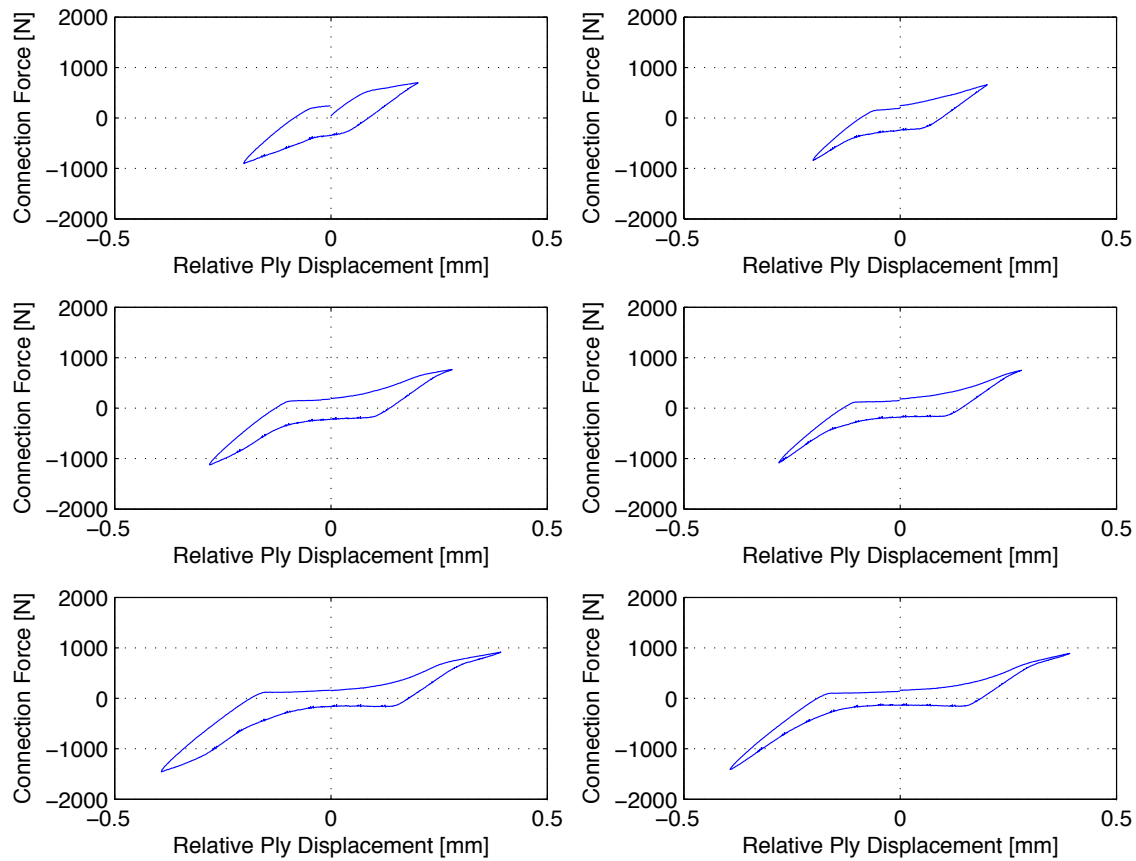
Picture 5.3.1.2. – Load displacement behavior WW6-33HEX10 cyclic test

Picture 5.3.1.3 shows the mechanism and the difference between a push and a pull test. On the left side the mechanism of a pull test can be seen, the right side shows the mechanism of a push test.

It was observed that during the pull parts the studs were pressed together at the connection. The ends of the studs were separating. As a result of this mechanism, the connection seems to be under pressure. During the push part the ends of the studs pressed against the studs and a separation started at the connection. This result is an additional load of the screw.
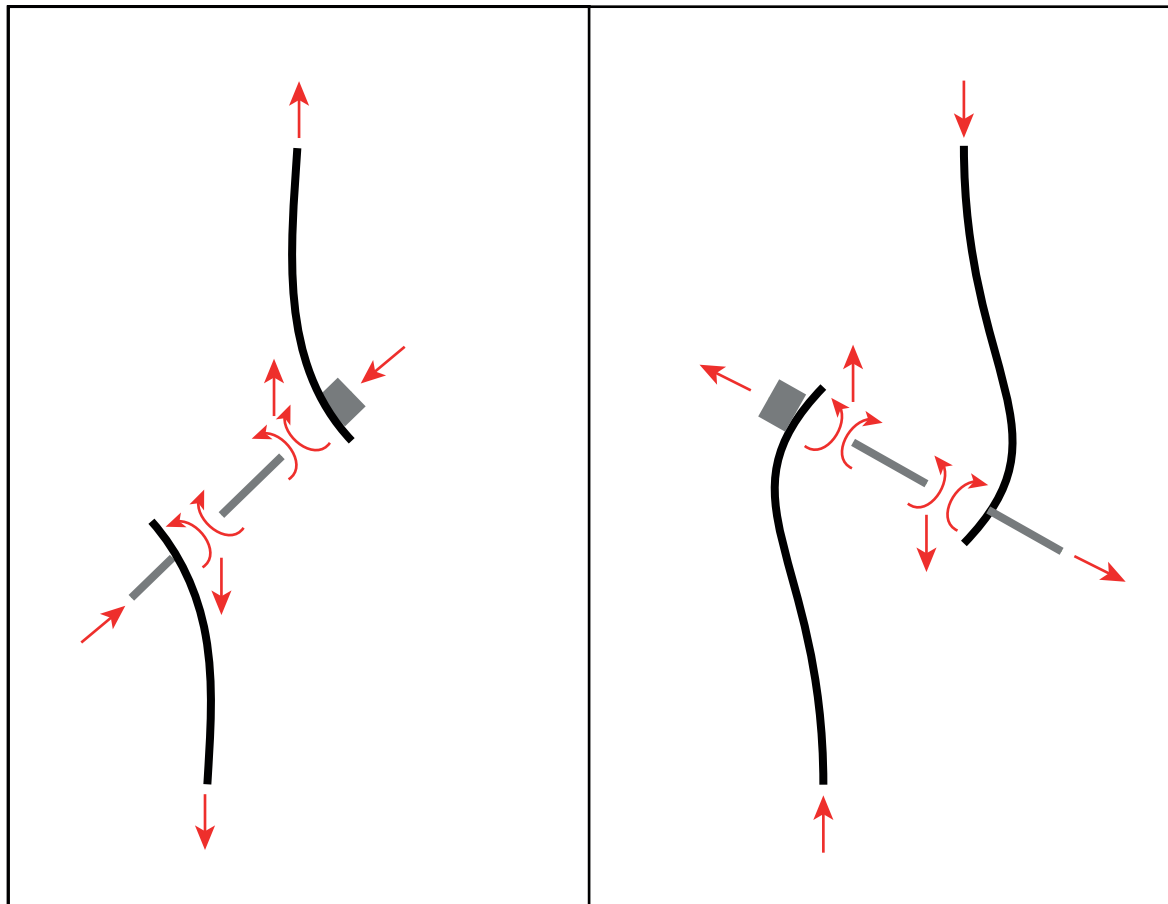
Picture 5.3.1.3. – Mechanism of the connection

These two mechanisms also explain the reason that the difference between the push and pull side is stronger for thinner connections. Stiff connections like #44 don't show such a distinctive deformation. It follows that the influence on the screw for thick connections is smaller than for thin connections like #33 with a strong deformation.

5.3.2. Influence of the Screw Size

While analyzing the monotonic tests, it was observed that different material thicknesses and different types of screws have an influence on the results. After discussing the influence of different material thicknesses on cyclic tests, it is interesting to look for the influence of different screw sizes on the load displacement behavior of the connection.

A first view at the results of the cyclic tests shows similar behavior for all screw sizes. The main difference was detected on the pull side. This difference shows mainly a lower stiffness of the #8 screws. The behavior of #10 and #12 screws are similar and do not differ significantly.
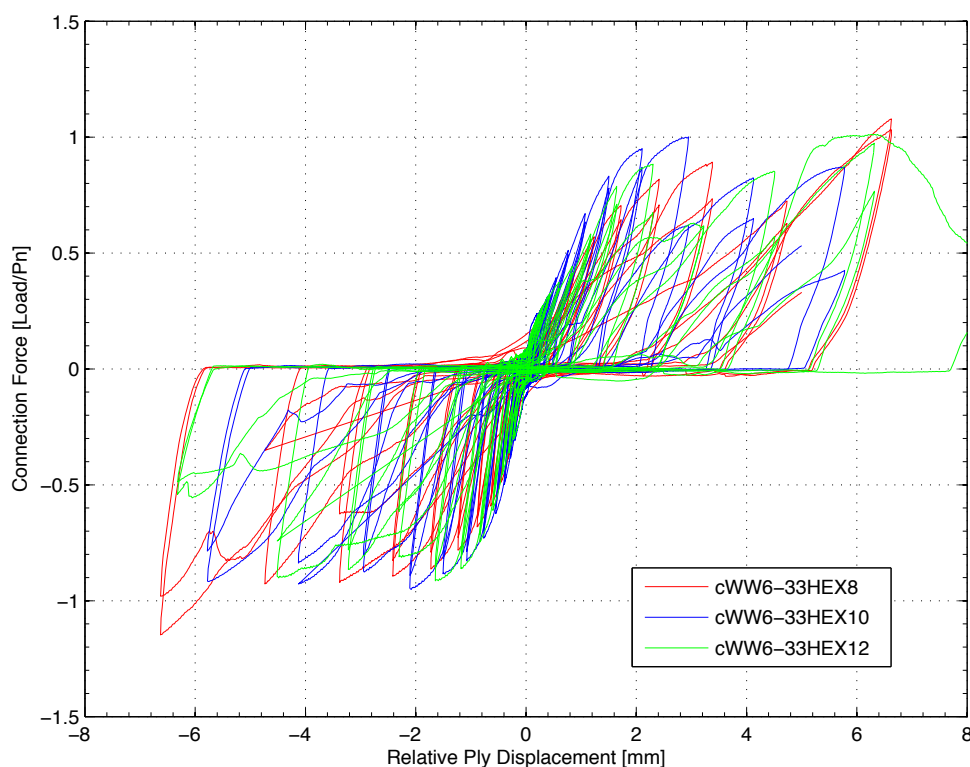
Picture 5.3.2.1. – Comparison of different screw sizes #33

A better impression of the influence of different screw sizes on the connection provides picture 5.3.2.2. While the difference of the stiffness is significant, the difference of the maximum load can clearly be seen. As a reminder for the monotonic tests, #103 connection tests only fail because of bearing and tearing. This concludes, that the influence of different screw sizes is stronger on bearing and tearing as on tilting. Bearing as a failure mode always showed a plastic deformation while testing. This explains why the maximum load for #8

screws is smaller than the maximum load for #10 or #12 screws. Because of the smaller diameter, the maximum strength will be reached before the other screws.
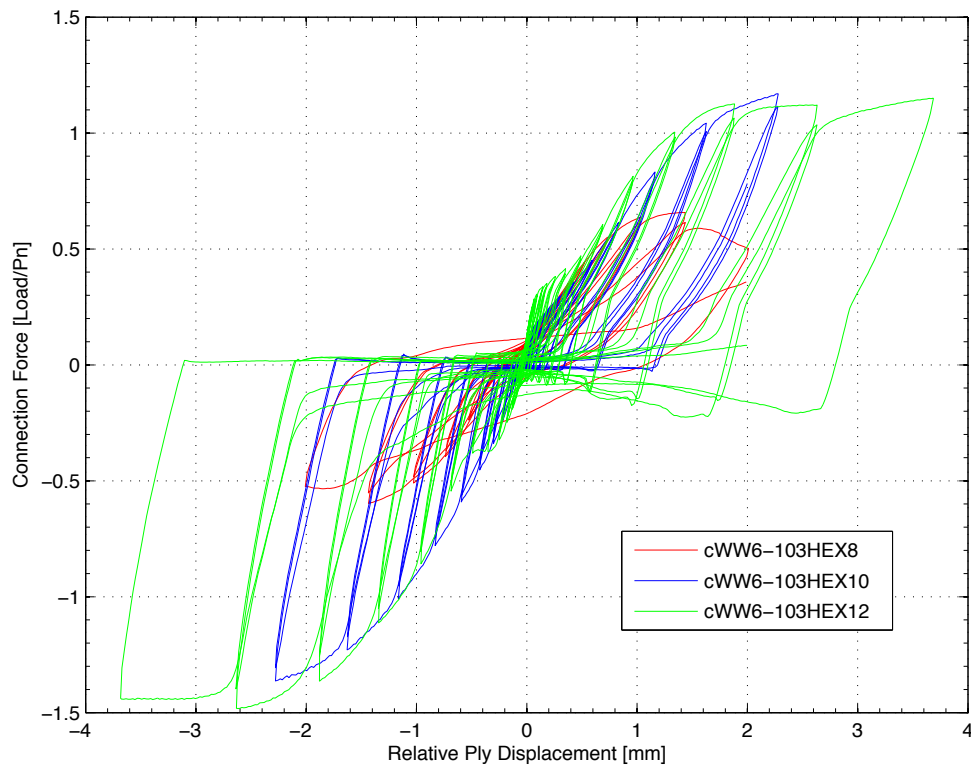
Picture 5.3.2.2. – Comparison of different screw sizes #103

Picture 5.3.2.3 gives a more detailed view of the #33 connection. It can be seen, that the behavior of #10 and #12 screws are similar. Especially on the pull side, the #8 screw shows a different behavior, which is caused by the test method. All the tests started with pulling the studs apart. For the #33 tests, the first failure mode is tilting. The first deformation is the most important deformation for this test. After increasing the hole of the screw, the resistance against rotation of the screw decreases. Changing the method to pushing together, there is a possibility for rotation. After the maximum rotation is reached, bearing starts. As it is presented in picture 5.3.2.2 as well as in the series of picture 5.3.2.3, the behavior for bearing is nearly the same.
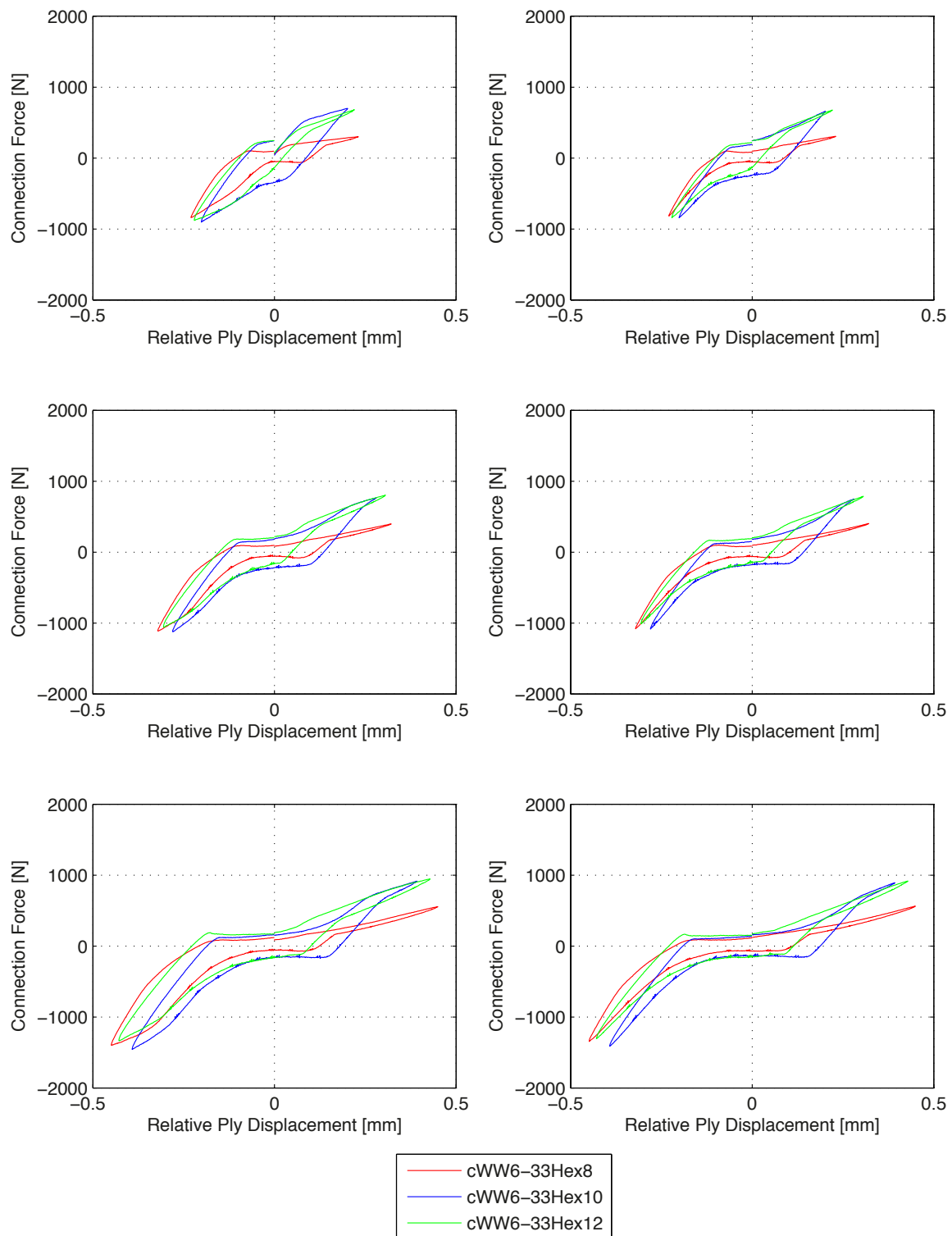
Picture 5.3.2.3. – Details of the first cycles

5.3.3. Compare monotonic and cyclic Testing

The last discussion of this research is the difference between monotonic and cyclic tests. Therefore the following pictures demonstrate the comparison of monotonic tests with the corresponding cyclic tests.

At it was determined, the curves for the monotonic and cyclic tests are the same at the beginning. But within a few cycles a separation of the monotonic and the cyclic tests follows. The load-displacement behavior of the monotonic tests is stiffer as long as tilting can be seen. At the point where bearing starts, which is in common the maximum load for the connection, the difference between monotonic and cyclic tests is getting closer.
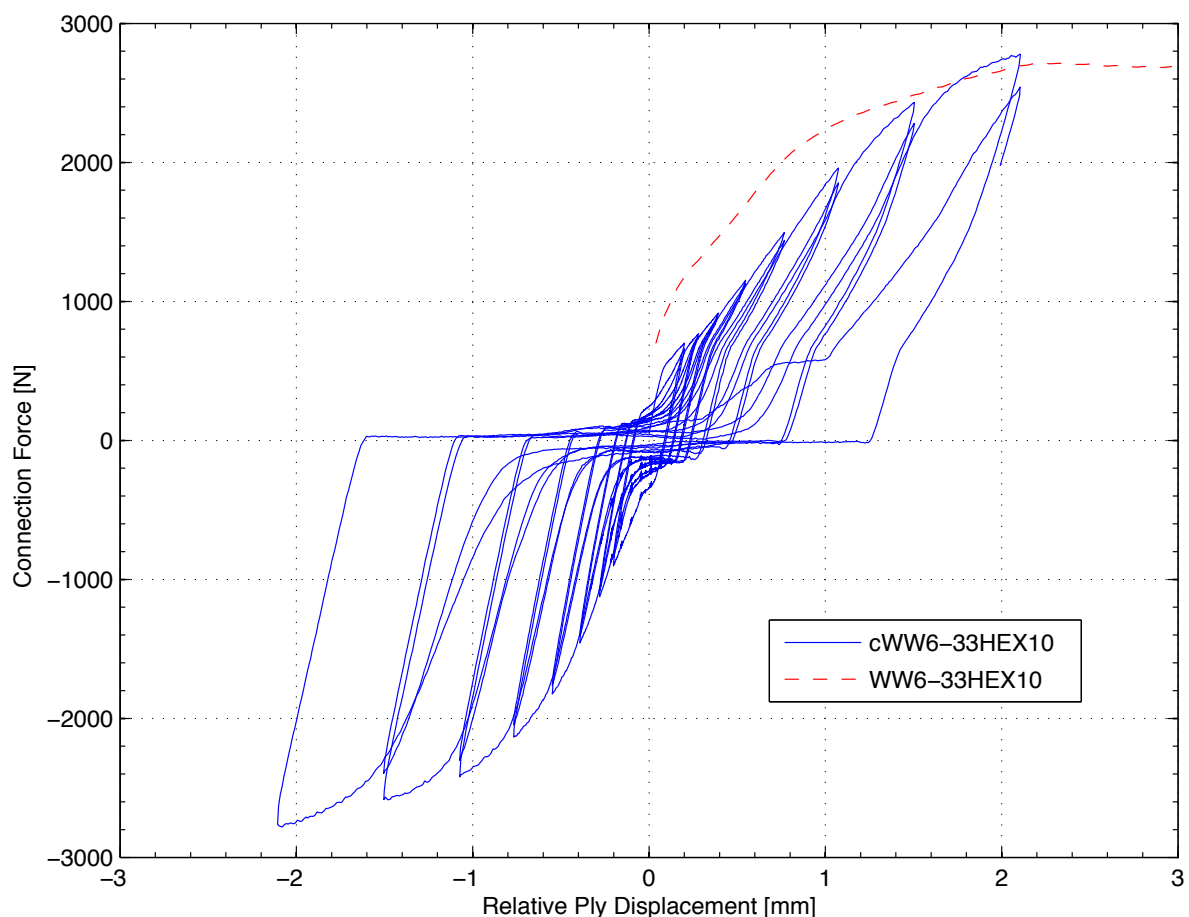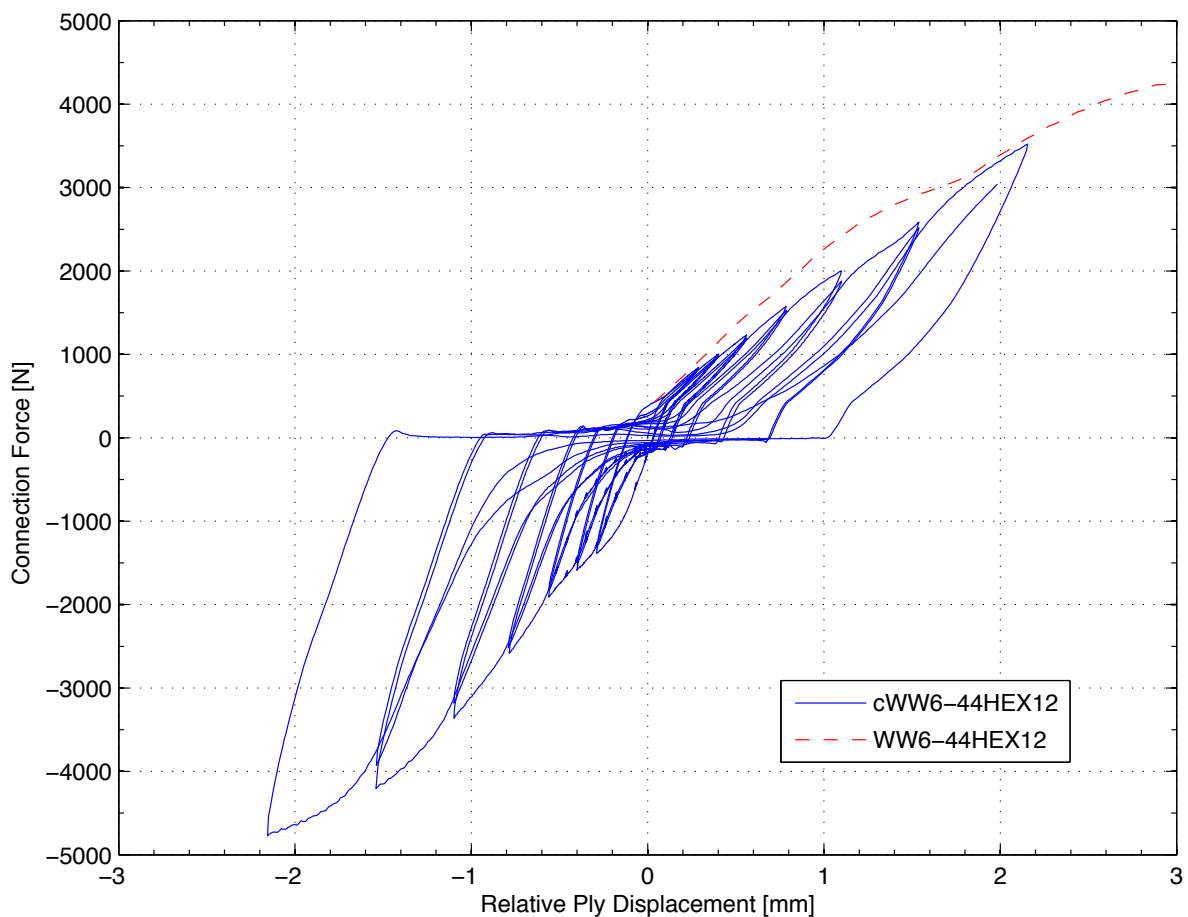

Picture 5.3.3.1. – Comparison of a #33 monotonic and cyclic test

That means, that tilting is more vulnerable to the influence of cyclic tests like the monotonic tests. This fact can also be seen in picture 5.3.3.3, which shows a comparison of #103 tests. As described before, the failure mode of such a connection is bearing.

It can be summarized, that there is a big difference between monotonic and cyclic tests, which occurs after the first few cycles.

The first cycle of a cyclic test is the same as in the beginning of a monotonic test. After unloading the system a small damage remains. When loading starts again, the hole of the screw is larger than be fore and the rotation of the screw starts delayed. That explains why the load-displacement behavior of a cyclic test is lower than a monotonic test. With increasing cycles the displacement becomes bigger and tilting goes over to bearing. At this point the rotation of the screw is done and the failure for monotonic and cyclic testing is the same with the same capacity.

Picture 5.3.3.2. – Comparison of a #44 monotonic and cyclic test
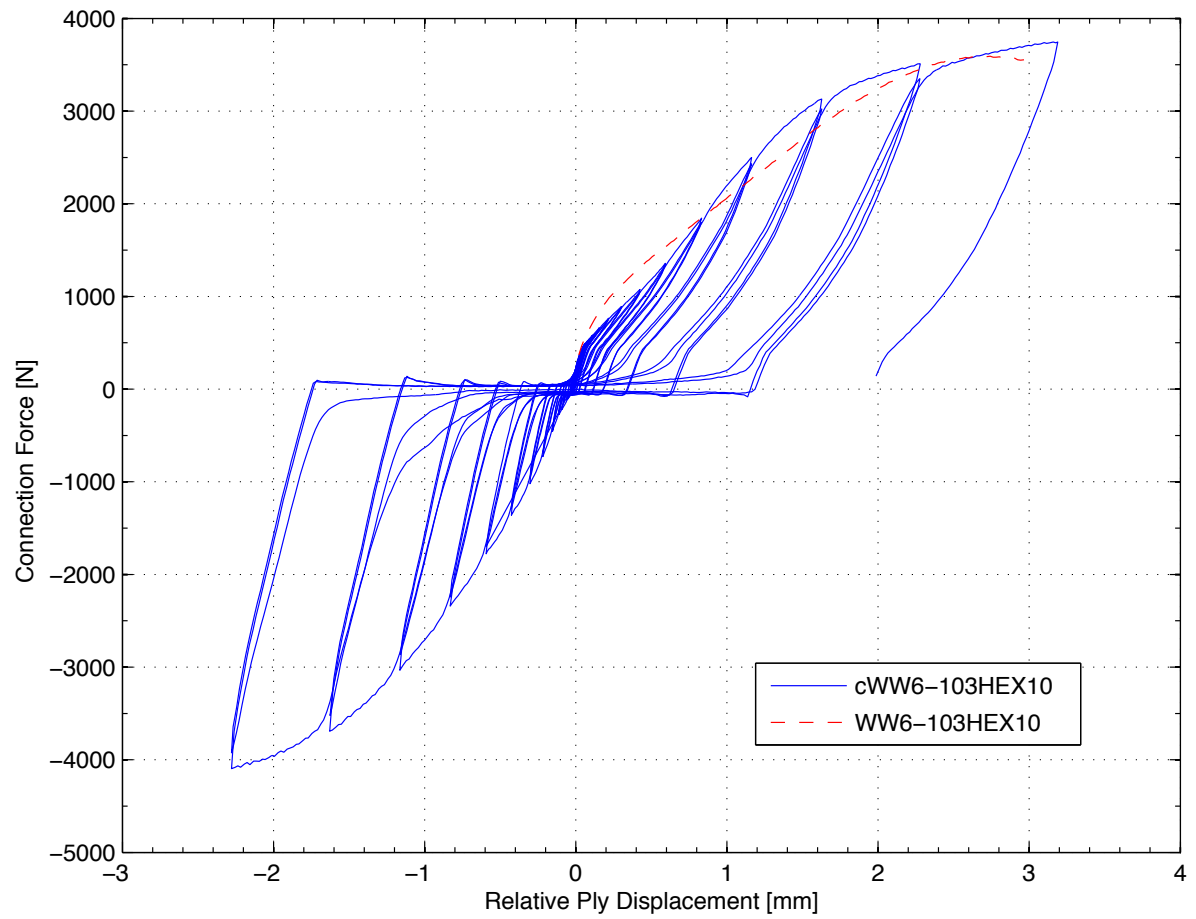
Picture 5.3.3.3. – Comparison of a #103 monotonic and cyclic test

6. Conclusions and Recommendations

6.1. Conclusions

The behavior of a cold-formed steel connection highly depends on its components. For this reason, an experimental test program was conducted in the structures laboratory of the Civil & Environmental Engineering Department of the Virginia Polytechnic Institute and State University including tests of tension monotonic and cyclic loading. The tested screws were selected in such a way, how often they were used for common constructions (Hex Washer Head, Truss Head, Pancake Head, Flatpan Head with sizes of #8. #10 and #12). Additionally, three connection pairs with two different orientations were included (0.88 mm to 0.88 mm (#33), 1.15 mm to 1.15 mm (#44) and 2.58 mm to 0.88 mm (#103) with the orientations web-to-web and web-to-flange). The conclusion obtained for the analysis of the monotonic test connection results were:

Szilard's equation for the plate theory shows good results compared to the conducted tests. In the beginning of the tests, as long as elastic behavior occurs, both plates of the connection can be seen as one thick plate. With the beginning of plastic deformation, the load-displacement behavior grows nonlinear. Therefore, for the calculation of the reference displacement the best results can be obtained by using only the thickness of the thinner plate.

The tested screw types differ from each other in the lower surface of the heads and their diameter. For the thin connections there was only a difference between the screws because of the lower surface. For thick connections, no different behavior was obtained.

The thickness of the screw influenced the failure mode of the connection. Thin connections (#33 and #44) have started with tilting. The thick connections (#103) have started with tilting. The stiffness of the #33 and #44 connections was the same and was higher than the stiffness of the #103 connections.

The influence's strength of the connection orientation depends on the thickness. #33 connections show a difference of the stiffness. For #44 and #103 connections no difference between web-to-web and web-to-flange connections was obtained.

The conclusion obtained for the analysis of the cyclic test connection results were:

The cyclic tests show a difference on the push and pull side of the load-displacement behavior. It was found out that the push side shows higher loads than the pull side. This difference of loads is caused by a difference of the mechanism of the connection. The influence of the connection mechanism is stronger for #33 connections than for #103 connections and depends on the thickness of the studs.

The load-displacement behavior of monotonic and cyclic tests in the beginning is similar. With starting of plastic deformation and additional cycles, a separation of monotonic and cyclic tests starts with a higher stiffness of the monotonic tests.

6.2. Recommendations

The whole test setup is very specific for two types of connections, the web-to-web and the web-to-flange connections. Each type of connection has its own specific boundary conditions and both connections can't be seen as a general setup for all possible connections. As it can be followed from the interpretation of the monotonic tests, the area of influence on the connection is close to the screw and is not strongly influenced by the edge distance of the used test setup, but is highly influenced by the connection type and thickness.

Even if the results of each combination are similar, there is still a big variation of many parameters like steel thickness and steel strength. Another test series to evaluate this variation is to approve.

For future a more general test setup with a bigger variation of different thicknesses should be tested. This information would be helpful to characterize the behavior under cyclic loading, especially for the difference of the pull and push side.

For this test series only single screw connections were tested, even if the common connection in cold-formed steel uses more than one screw. The interaction of a multi screw connection was not considered and must be proved separately

The main object of this research is to analyze the difference of the energy dissipation of connections under monotonic and cyclic loading. The results show, that the failure modes of the AISI S100 do not work for cyclic testing. Especially after a few cycles a significant

difference between the monotonic and cyclic tests was determined. For this part the equations of the AISI S100 must be transformed and adapted to the cyclic tests or new equations, which consider the characteristic behavior of connections under cyclic loading.

7. References

[1]   Padilla, D., Cyclic Energy Dissipation of Cold-Formed Steel Studs - Experiencing Euler Buckling, Structures Congress 2012 © ASCE 2012, p. 1518, 2012.

[2]   Okasha, A., Performance of steel frame / wood sheathing screw connections subjected to monotonic and cyclic loading, McGill University, Canada, 2004.

[3]   Peterman, K. D., Nakata, N., Schafer, B. W., Cyclic Behavior of Cold-Formed Steel Stud-to-Sheathing Connections, 15 WCEE, Lisboa 2012, 2012.

[4]   Okasha, A., Performance of steel frame / wood sheathing screw connections subjected to monotonic and cyclic loading, McGill University, Canada, p. 24, 2004.

[5]   Okasha, A., Performance of steel frame / wood sheathing screw connections subjected to monotonic and cyclic loading, McGill University, Canada, p. 27, 2004.

[6]   Krawinkler, H., Loading Histories for cyclic tests in support of performance assessment of structural components. p. 1, 2009.

[7]   Padilla, D., Cyclic Energy Dissipation of Cold-Formed Steel Studs - Experiencing Euler Buckling, Structures Congress 2012 © ASCE 2012, p. 1518, 2012.

[8]   Krawinkler, H., Loading Histories for cyclic tests in support of performance assessment of structural components. p. 3, 2009.

[9]   Krawinkler, H., Loading Histories for cyclic tests in support of performance assessment of structural components. p. 3-6, 2009.

[10]   Krawinkler, H., Parisi, F., Ibarra, L., Ayoub, A., Medina, R., Development of a Testing Protocol for Woodframe Structures, 200b, CUREE Publication No. W-02.

[11]   Applied Technology Council Interim Testing Protocols for Determining the Seismic Performance Characteristics of Structural and Nonstructural Components, FEMA 61, 2007.

[12]   Krawinkler, H., Loading Histories for cyclic tests in support of performance assessment of structural components. p. 5, 2009.

[13]   Szilard, R., Theories and Applications of Plate Analysis: Classical, Numerical and Engineering Methods, John Wiley & Sons, Inc., p. 98, 2004.

[14] Szilard, R., Theories and Applications of Plate Analysis: Classical, Numerical and Engineering Methods, John Wiley & Sons, Inc., p. 99, 2004.

[15] Szilard, R., Theories and Applications of Plate Analysis: Classical, Numerical and Engineering Methods, John Wiley & Sons, Inc., p. 31, 2004.

[16] Padilla, D., Cyclic Energy Dissipation of Cold-Formed Steel Studs - Experiencing Euler Buckling, Structures Congress 2012 © ASCE 2012, p. 1520, 2012.

[17] http://www.clarkdietrich.com/sites/default/files/imce/pdf/SupportDocs/Productinfo/CD_Product_Identification.pdf, 07/26/2012.

[18] MTS, Manual – Using TestWorks4, p. 27, 2011.

[19] American Iron and Steel Institute, AISI STANDAED 100-2007-C, p. 130-132, 2007.

[20] American Iron and Steel Institute, AISI STANDAED 100-2007-C, p. 100, 2007.

[21] http://www.strongtie.com/ftp/catalogs/c-fs11/C-FS11_p182.pdf, 08/01/2013.

8. Eidesstattliche Erklärung

Abschlussarbeit von:

Herrn Andreas Haus

Erklärung zur Abschlussarbeit gemäß §23, Abs. 7 APB

Hiermit versichere ich, die vorliegende Abschlussarbeit ohne Hilfe Dritter nur mit den angegebenen Quellen und Hilfsmitteln angefertigt zu haben. Alle Stellen, die aus den Quellen entnommen wurden, sind als solche kenntlich gemacht worden. Diese Arbeit hat in gleicher Form oder ähnlich Form noch keiner Prüfungsbehörde vorgelegen.

Münster, den 17.12.2013

Andreas Haus